The Thesis Committee for Maite Bizcarguenaga Doucet
Certifies that this is the approved version of the following Thesis:

Evaluating the cooling potential of vertical greenery systems in urban residential areas to mitigate urban heat island, reduce energy loads, and improve thermal comfort conditions in a hot humid climate.

APPROVED BY
SUPERVISING COMMITTEE:

Juliana Felkner, Supervisor

Katherine Lieberknecht

Evaluating the cooling potential of vertical greenery systems in urban residential areas to mitigate urban heat island, reduce energy loads, and improve thermal comfort conditions in a hot humid climate.

by

Maite Bizcarguenaga Doucet

Thesis

Presented to the Faculty of the Graduate School of

The University of Texas at Austin

in Partial Fulfillment

of the Requirements

for the Degree of

Master of Science in Sustainable Design

The University of Texas at Austin

May 2021

Acknowledgements

First and foremost I am extremely grateful to my supervisor, Professor Juliana Felkner, whose expertise was invaluable in formulating the research question and methodology, and to my second reader, Professor Katherine Lieberknecht, whose feedback was instrumental to this research. Their insightful comments and suggestions pushed me to sharpen my thinking and brought my work to a higher level. This study would not have been accomplished without their endless support, knowledge, and patience.

I would like to express my sincere gratitude to my family, particularly my aunt and uncle, Nadine and Christian, for driving me all the way to Texas, and for always being there when I need them. To my wife´s family, for their constant friendship and support. Austin would not be the same without them.

To my brothers, Ander and Iker, for always being there to make me laugh and for their never-ending support. For their presence in the most difficult times. Thank you for always being there.

To my father, Bosco, and my mother, Cécile, who I miss the most, for their love, unwavering support, and belief in me. Thank you for giving me the opportunities and experiences that have made me who I am, and for providing me with the tools I needed to get here.

And finally, I am deeply grateful to my wife, Rocio, for providing me with unfailing support and continuous encouragement. This accomplishment would not have been possible without your endless love and devotion. Thank you.

Abstract

Evaluating the cooling potential of vertical greenery systems in urban residential areas to mitigate urban heat island, reduce energy loads, and improve thermal comfort conditions in a hot humid climate.

Maite Bizcarguenaga Doucet, M.S.S.D.

The University of Texas at Austin, 2021

Supervisor: Juliana Felkner

This master´s thesis aims at studying the summer cooling effects of green walls to reduce urban heat island effects, improve thermal comfort, increase the potential of natural ventilation, and reduce buildings' cooling loads. Using ENVI-met model simulations, this study investigated the influence of green facades on the ambient air temperature and its role on the air fluctuations in the hot humid climate of Austin at a neighborhood and a building scale, with a primary focus on residential buildings. The results show adding green facades mostly impact the surface temperature during the hottest hours of the day, registering a maximum surface temperature reduction of 5.21°C. The simulation results also indicate small air temperature reductions in the afternoons reaching a maximum reduction of 0.23°C, and slight air temperature increases during the night showing a maximum value of 0.20°C. These findings can provide architects, designers, planners, and policymakers with a better understanding of the many benefits greenery and particularly green facades have, and provide them with the necessary tools to implement new solutions

across sectors and scales to reduce the impacts urban areas have on the environment, and provide a better living for all.

Table of Contents

List of Tables

List of Figures

Chapter 1: Introduction

Our planet is heating up fast. The average global temperature on Earth has increased by a little over 1°Celsius (2°Fahrenheit) since 1880, with two-thirds happening since 1975 (NASA, 2020). This unequivocal warming is primarily caused by increased greenhouse gas emissions resulting from human activities and the burning of fossil fuels (coal, oil, or gas) releasing gasses that trap the heat from the sun, increasing the temperature and causing long-term changes to our environment (Karl, Melillo, & Peterson, 2009; AAAS, 2009). Today, the world is already facing the visible signs of climate change, with increasing frequency and intensity of extreme weather events making it clear climate change possess a serious threat to humans and other species' health and wellbeing.

The growing population density is exacerbating the environmental degradation and presenting numerous challenges to humans and other species' survival. With fifty-five percent of the world´s population living in urban areas, a tendency that is expected to increase to sixty-eight percent by 2050 (United Nations, 2018), the assessment and improvement of urban environments is imperative. As cities increase their built-up area and expand to accommodate more people, space for nature is diminishing, inevitably disturbing the city´s ecological structure and contributing to the phenomenon known as Urban Heat Island (UHI) to occur (Akbari & Kolokotsa, 2016). Urban warming increases the frequency of extreme temperature events leading to the death of many people each year (WHO, 2018), and has serious impacts on the peak and total electricity demand in buildings primarily due to increased cooling loads (Santamouris, 2014). Cities worldwide generate seventy to ninety percent of carbon emissions (Douglas & James, 2015), and buildings account for thirty-two percent of the energy used and nineteen percent of energy-related greenhouse gas emissions (Hawken, 2017), further contributing to climate change.

Reducing these impacts is essential for building more sustainable cities, and reducing people´s exposure to extreme weather.

For this reason, the purpose of this master´s thesis is to mitigate UHI to reduce buildings' thermal energy loads and improve thermal comfort conditions in urban residential areas, by evaluating the cooling potential of natural ventilation integrated with vertical greenery systems. Because it is not only important to shape the way we build and design the structures to come, but it is vital we fix current buildings, this work also reviews how to noninvasively retrofit residential buildings to improve their thermal performance using passive design strategies, looks into the lessons learned from vernacular architecture regarding the use of natural ventilation and vegetation as positive thermal regulators, and analyzes the additional benefits these improvements can have on people and the environment.

Chapter 2: Literature Review

In this chapter, the theoretical basis for my analysis is reviewed. I begin with defining the UHI effect, its causes, effects, and mitigation strategies, followed by a presentation of greenery systems, introducing green roofs and green walls, explaining their benefits and disadvantages, and finally stating the principles of bioclimatic design, understanding the changes in architecture design caused by the introduction of air conditioning and peoples' thermal expectations.

URBAN HEAT ISLAND

In addition to an already warming planet, cities are further impacted by the Urban Heat Island (UHI) effect (Rouviere, et al., 1990). UHI is defined as higher temperatures registered in urban areas than in their corresponding surrounding suburban and rural areas (Oke, 1982). Evidence showing this phenomenon was first provided by Luke Howard in 1818, who measured and compared the temperature in London and its surrounding countryside (Howard, 1833) and has been widely observed and researched around the world ever since (Huang & Lu, 2017; Yow, 2007). It is one of the most documented climatological effects of human´s impact on the environment (Oke, 1973).

UHI is a result of urbanization and has many impacts on human and natural systems. Amongst other things, the UHI effect is caused by land-surface modifications affecting the storage and transfer of heat, water, and airflow, and by anthropogenic heat released from buildings, vehicles, and human activity (Santamouris, Chapter 5: Heat-Island Effect, 2001; IPCC, 2013). Studies have found that the heat re-radiated by the urban surfaces plays the most important role (Memon, Leung, & Chunho, 2007) as the thermal and hydrological properties of the materials used in buildings and cities' physical infrastructure differ greatly from the properties of soil, trees, and plants, heating far more than vegetated surfaces in direct sunlight (Douglas & James, 2015). For example, on a hot day, conventional rooftops can sustain temperatures of up to 90° Celsius (162° Fahrenheit) higher than the air around them, contributing to the UHI effect and increasing the cooling loads of the floors below (Hawken, 2017).

Furthermore, the color, roughness, and composition of urban materials contribute to the formation of UHIs. The urban fabric and low albedo materials absorb and store heat from the sun throughout the day and release it slowly during the night, increasing the UHI intensity particularly at night (Oke, 1982). Darker materials with a lower albedo absorb and retain more heat than light-colored surfaces, and as presented in (Santamouris, 2013), numerous studies have been performed to correlate the impacts different colored materials have on their surface temperature and sensible heat release. Additionally, sidewalks, roads, roofs, and other hard dry urban surfaces provide less moisture than natural and vegetated surfaces contributing to higher temperatures affecting the thermal balance of cities (EPA, n.d.).

The intensity of UHIs, which is the maximum temperature difference registered between the urban area and its surroundings, varies in different locations and throughout the day depending on the climate zone, the urban form, and the building density and characteristics (Oke, 1982). Studies have shown the highest intensity is often reached between eleven o'clock at night and three o'clock in the morning (Douglas & James, 2015), and numerous experimental data show the UHI intensity varying between 0.5° Celsius (0.9° Fahrenheit) and 11° Celsius (19.8° Fahrenheit) with an average maximum value between 4.1° Celsius and (7.4° Fahrenheit) 6° Celsius (10.8° Fahrenheit) (Santamouris, 2019). Further studies have concluded that the UHI intensity is highly reduced during rainy days, that high relative humidity corresponds to a lower UHI intensity, and that coastal cities have a considerably lower UHI intensity (Santamouris, 2015).

Now, Voogt and Oke (2003) explain that UHIs can be determined on different layers of the urban atmosphere, and for various surfaces, resulting in different types of UHIs. The two main types are the canopy layer UHI determined by the air temperature, and the surface UHI (Schwarz, Lautenbach, & Seppelt, 2011). These differ in the way they are measured, how they are formed, their characteristics, and their impacts (EPA, n.d.; Sheng, Tang, You, Gu, & Hu, 2016). Figure 1 illustrates the difference between the surface and air temperatures during the daytime and nighttime in different urban and rural settings.

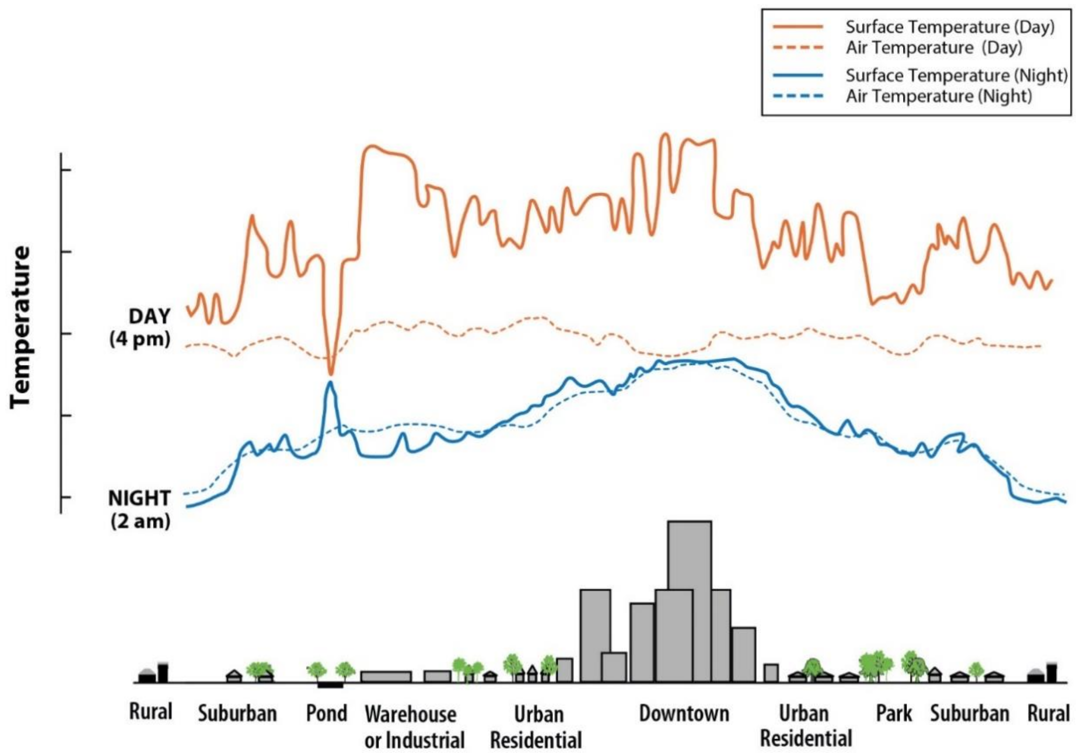

Figure 1: Urban Heat Islands. (USGS, 2019)

Urban warming has a significant impact on the global energy consumption of buildings predominantly due to cooling purposes (Santamouris, 2014), and is also associated with increasing the intensity and duration of heatwaves (Ward, Lauf, Kleinschmit, & Endlicher, 2016), worsening the air quality (WHO, 2018), deteriorating thermal comfort (Santamouris, 2015), affecting people´s health and well-being (Heaviside, Macintyre, & Vardoulakis, 2017; Franchini & Mannucci, 2015), raising CO2 emissions, and affecting biodiversity. Important research aiming to understand the effects of UHI has been carried out in the past decades, and studies presenting mitigation strategies such as the use of vegetation, increasing evapotranspiration, and increasing solar reflectance have recently augmented (Huang & Lu, 2017; Andoni & Wonorahardjo, 2018; Akbari & Kolokotsa, 2016). It is important to continue these efforts to better understand how to mitigate the effects of UHI and provide cities with proper guidelines and a wide range of potential solutions.

GREENERY SYSTEMS

Green areas can provide many environmental benefits such as reducing greenhouse gas emissions, air and noise pollution (Radic, Dodig, & Auer, 2019), UHI (Andoni & Wonorahardjo, 2018), acidic rain, water runoff (Sedlak, 2014), and improve thermal comfort, human health and well-being (Hartig & Kahn Jr., 2016; Tzoulas, et al., 2007; Elsadek, Liu, & Lian, 2019), and enhance biodiversity (Douglas & James, 2015). Depending on many factors such as soil cover, the density of plan coverage, and the building's materials, green walls, and green roofs can also improve both a building´s heating and cooling performance, and the outdoor temperature (Besir & Cuce, 2017; Li, Wei, & Li, 2019), and improve the environmental impact of buildings (Radic, Dodig and Auer 2019).

However, with fifty-five percent of the world´s population living in urban areas (United Nations 2018) and as cities expand to accommodate more people, space for nature is decreasing (Standish, Hobbs and Miller 2012). Research conducted in four metropolitan areas in the USA by Akbari and Rose (2007) shows that on average vegetation covers 20 to 37% of the area, roofs 20 to 25%, and paved surfaces 29 to 36%, demonstrating hardcover surfaces predominance. This is placing much pressure on urban green areas to conserve biodiversity, protect water resources, control microclimates, and improve human health and well-being (Lovell and Taylor 2013). Different solutions across sectors and scales need to be implemented in cities today for a more resilient and sustainable future.

As a result of technological breakthroughs coupled with increasing proof of their many benefits, green walls and roofs have gained popularity around the world, and some countries are changing their policies and regulation to promote or mandate the use of greenery systems in new buildings. San Francisco, for example, was the first city in The United States to adopt a green roof mandate in 2016 (Hawken, 2017). Now, there are many different types of greenery systems and a proper understanding of each one is needed to comprehend their features and distinctions so they can be adequately implemented.

Green roofs and walls are not contemporary concepts; they are an evolving human invention and their history goes back thousands of years (Jim 2017). The earliest recorded example is the Hanging Gardens of Babylon built around 500 BC, and other buildings covered with vegetation were also found in the Roman and Greek empires (Besir and Cuce 2017). Climbing plants were particularly used in the Mediterranean region to protect buildings from sunlight and provide thermal insulation, and their use was greatly expanded in Europe and North America during the 19th century as ornamental elements (Besir and Cuce 2017). Starting from vernacular traditions green roofs began as a practical solution for people living in harsh environments with climatic extremes and have developed through time (Jim 2017).

Green roofs

Roofs account for 20 to 25% of urban surfaces, increasing green roofs' potential to positively affect the urban environment (Besir and Cuce 2017). Green roofs are composed of a series of layers finished with growing medium and vegetation installed on a roof surface, and are often divided into three categories: extensive, semi-intensive, and intensive (Vijayaraghavan 2016, Besir and Cuce 2017, Raji, Tenpierik and Van Den Dobbelsteen 2015). The different layers must be carefully designed to ensure the roof itself is protected, and plants can thrive (Hawken, 2017) knowing that roofs are not favorable environments for plants to grow.

Extensive green roofs have a shallow layer of a growing substrate of fewer than twenty centimeters deep, supporting a limited variety of plant species, and are light-weighted, low-cost, and require little maintenance (Raji, Tenpierik and Van Den Dobbelsteen 2015, Besir and Cuce 2017). The semi-intensive green roofs have a slightly deeper layer of growing substrate, supporting low-growing plant species, and intensive green roofs have a deep layer of growing substrate, supporting a wider variety of plant types, but are heavier, more expensive, and require more maintenance (Besir and Cuce 2017, Raji, Tenpierik and Van Den Dobbelsteen 2015, Baciu, Lupu and Maxineasa 2019). Due to weight restrictions, costs, and maintenance, extensive green roofs are more common worldwide (Vijayaraghavan 2016).

As suggested before, greenery systems provide many benefits, but green roofs, in particular, can reduce stormwater runoff by reducing the amount of water and the speed at which it leaves a property and enters the sewer (Sedlak, 2014). Additionally, green roofs are highly effective at insulating the floor below, thus reducing the amount of energy buildings need for cooling and heating (Besir and Cuce 2017, Green Roofs for Healthy Cities 2019). Most of these benefits are directly correlated with the substrate composition and thickness (Shafique, Kim and Rafiq 2018), and research shows higher water retention and thermal benefits with the increased thickness of the growing medium layer (Besir and Cuce 2017).

Unfortunately, many green roofs get proposed and designed, but only a few in comparison get installed, in part because they add to the cost of the building (Sutton 2018). Additionally, green roofs add to the load of the roof structure, limiting the number of buildings that can be retrofitted without having their structure modified to support the installation (Cascone, et al. 2018). A study on a multi-story residential building located in Catania, Italy, found that only a few green roof solutions with a maximum thickness of 10 centimeters using limited substrate combinations were suitable for the retrofitting of the existing buildings (Cascone, et al. 2018). Many elements need to be revised and considered before installing a green roof on a new or existing construction, and the structure's load-bearing capacity must be revised and calculated by a structural engineer. In the end, the added weight, and installation and maintenance costs can be limiting factors to their installation (Baciu, Lupu and Maxineasa 2019).

Green Walls

Green walls have an even greater potential at saving valuable floor real estate than green roofs since façade surfaces can be in some cases far larger than the size of the roof (Manso and Castro-Gomes 2014). The term green wall refers to all forms of vegetated vertical surfaces (Green Roofs for Healthy Cities 2019) and can be located inside or outside a building given the proper conditions. Depending on the system, these systems can also be proposed on inclined surfaces. Green walls can be divided into two main categories which are green facades and living walls, and further subcategorized into their different systems (Manso and Castro-Gomes 2014, Besir and Cuce 2017). Figure 2 shows the different categories and subcategories of green wall systems proposed by Manso and Castro-Gomes (2014).

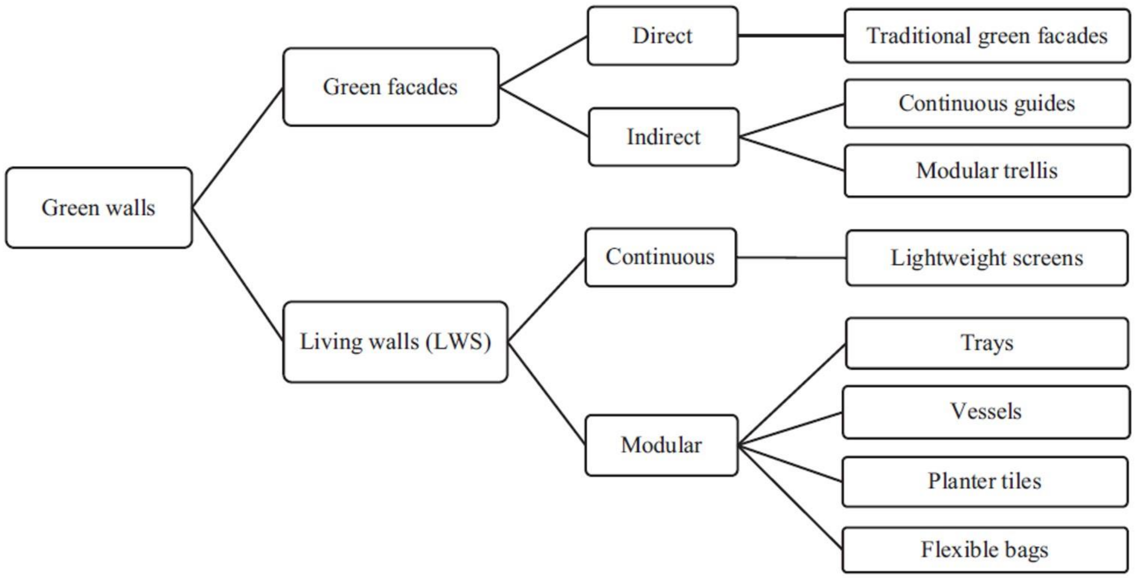

Figure 2: Classification of green walls, according to their construction characteristics (Manso & Castro-Gomes, 2014)

Green facades are based on the application of climbing or hanging plants along a wall and can be subcategorized as direct green facades, where plants are attached directly to the wall, or indirect green facades, where a supporting structure is needed for the vegetation to grow on (Manso and Castro-Gomes 2014). Of all the greenery systems, green facades have the smallest environmental burden since only a few materials are needed for their installation and maintenance (Manso and Castro-Gomes 2014, Jim 2017). Other than the already mentioned benefits, in comparison with living walls, green facades are less likely to detach from the wall or support system, light-weight training or support systems can be mounted directly on and be supported by most walls, they have a lesser chance of weed invasion, consumes less water and need a simple irrigation system at the foot of the wall, and don’t require complex filtration and water quality standards, and are easy and not expensive to install or maintain (Jim 2017). However, the choice of species is very limited, it may take longer to cover a wall, they have a relatively low thermal insulation factor, have a lesser cooling effect due to evapotranspiration and shading, and are less effective at combating air and noise pollution (Jim 2017).

Climbing plants and in particular self-clinging climbers are often thought to be harmful to a building’s surface. Some climber species have aggressive roots and can damage a wall surface if it has cracks or openings, and are not recommended for wood or composite sidings since they hold moisture which can eventually rot the façade (Mather 2017, Marcus 2010). However, they have been used for centuries, and research shows that on adequate materials and in proper conditions, climbing walls can be beneficial and protect the building’s façade (Sternberg, Viles and Cathersides 2010, Marcus 2010, Mather 2017). A study on the role of ivy (*Hedera helix*) on historic stone walls in different climatic zones in England demonstrated that ivy functions as a mechanism to moderate temperatures and the effects of extreme climate, and contributes to the wall’s conservation (Sternberg, Viles and Cathersides 2010). Self-clinging climbers can provide additional benefits, and in proper conditions, there is no reason for damage to occur.

Living walls are modern systems where pre-vegetated panels are mounted on a structural wall or free-standing frame (Green Roofs for Healthy Cities 2019), and have gained popularity in recent years particularly as a way of integrating vegetation in tall buildings. They can be categorized as continuous and modular, where the main difference is the growing media as continuous systems use a geotextile membrane instead of soil using hydroponic techniques (Besir and Cuce 2017). Modular living walls usually come in the form of trays, vessels, planter tiles, or flexible bags, and differ in weight, composition, structure, assembly, and overall system (Manso and Castro-Gomes 2014).

In comparison with green facades, living walls perform well in full sun, shade, interiors, and different climates, because they support a greater diversity of low-growing plant species (Green Roofs for Healthy Cities 2019). Furthermore, living walls can rapidly achieve full cover as plants are pre-grown, have a low probability of plant roots to invade wall cracks, provide more effective thermal insulation and enhance the cooling effect due to evapotranspiration and shading, and they are more effective at improving air quality and controlling noise pollution (Jim 2017). Nevertheless, they are heavy, can fall in strong wind or heavy rain, have a higher probability for vegetation to perform poorly, more chance for weed invasion, require more water and complex irrigation systems often demanding high standards for filtration and water quality, require a moisture barrier, and are overall more elaborate and expensive to install and maintain (Jim 2017).

Green roofs and green walls

Technological advancements have expanded the possibilities for adding vegetation to the built environment which has been proven to be beneficial, especially to congested urban areas. Greenery systems have been used for centuries primarily as a way of protecting a building's envelop from harsh environments, and provide thermal insulation (Jim 2017, Manso and Castro-Gomes 2014). Today, green roofs and green walls are becoming increasingly popular for their aesthetic functions, and many studies show the many benefits they have on buildings, humans, and the environment. Unfortunately, most green roofs and living walls are hard to install and maintain, are expensive, and the load-bearing capacity of a building's structure may be insufficient to support such systems. Additionally, more materials with a higher environmental footprint for manufacturing are needed to build and maintain them (Manso and Castro-Gomes 2014).

Green facades, on the other hand, may not be as efficient as living walls at providing better thermal insulation, noise and air pollution reduction, and microclimate control, but they don't require complex irrigation systems, are less expensive, and easier to install and maintain. Regrettably, with much attention being devoted in recent years to living walls coupled with the popular belief of green facades harming the building's envelope, this natural solution for increasing the vegetated surface has not been sufficiently proposed and incorporated into new designs to cause a significant impact on urban environments.

Green roofs and green walls add to the load of the building structure, limiting the number of buildings that can be retrofitted without having their structure modified to support the installation and the number of developers who are willing to pay the cost of the additional structural requirements. Now, green facades are lighter (Jim 2017) and some climbing plants are known to grow horizontally especially when adequately trained, increasing the possible uses and applications of these plants.

Understanding the overall needs and limitations of every system is crucial to their success, and adequately assessing the location, plant species, greenery system, and building conditions can lead to better designs and solutions. Keeping in mind cities today struggle to provide sufficient water to satisfy their population's needs (United Nations 2019), and that projections show a forty percent water shortage by 2030 (Koop, Dorssen and Brouwer 2019), greenery systems must reduce their water consumption, a goal that can be attained by choosing native and drought-resistant vegetation (Jim 2017).

Conclusively, greenery systems can provide numerous benefits to humans and other species, buildings, and other infrastructure, and finally to the environment. New technologies have widened the possibility of adding more vegetation to the built environment. Given these system´s limitations, it is important to continue finding and evaluating different solutions of properly adding more vegetated surfaces in cities, and for architects, designers, planners, and policymakers to continue pushing for their implementation.

PASSIVE DESIGN STRATEGIES

Maintaining a tolerable indoor air temperature in overpopulated cities has proven to be challenging, and as a result, many buildings rely on electro-mechanical ventilation systems. In the United States, the residential sector accounts for 16% of the total energy consumption (Francis, 2019) of which 32% can be attributed to air conditioning and space heating (Woodward & Berry, 2018). Exposure to extreme temperatures contributes to human discomfort and health problems (Besir & Cuce, 2017) and leads to the deterioration of living environments and increases mortality rates. According to the Center for Disease Control and Prevention (CDC, 2017) about 618 people in the U.S. die of extreme heat every year, and they project the number of days above 37.8°C (100°F) to increase considerably, further stressing the need to implement solutions across sectors and scales to reduce people´s exposure to heat.

Many countries have imposed energy-saving policies on buildings and studies focusing on reducing the environmental footprint of buildings have emerged around the world (Panagiotidou & Fuller, 2013) as the need to reduce indoor temperatures, provide comfort, and protect vulnerable populations continue to increase (Santamouris, 2016). Mitigation strategies can be found in bioclimatic design and efforts should be directed towards learning and reincorporating these practices in today's architecture. The need for developing new products and technologies, educating architects, engineers, and the general public to follow these principles is imperative to move away from energy-dependent systems and create climate-adapted buildings with lower environmental impacts. It is important to revise the principles of bioclimatic architecture and its many benefits and understand the evolution of residential air conditioning and the thermal comfort expectations and regulations which have stirred architects away from bioclimatic design.

Residential Air Conditioning

Mechanical air conditioning units were first commercialized at the beginning of the twentieth century, soon after Willis Carrier, an American engineer and air-conditioning´s most recognized inventor and promoter (Ackermann, 2002) designed and installed a temperature and humidity control system for a printing company in New York (Nagengast, 2002). In the 1930s, despite substantial marketing efforts and people´s familiarity and affinity for this new technology, very few American residences were equipped with air conditioning units, and it was only between 1950 and 1980 that the industry saw a significant diffusion in residential air conditioning due to economic growth coupled with changes in the residential construction industry and favorable energy prices (Biddle, 2008). In the 1980s, almost 50% of American residences were equipped with air conditioning systems (Biddle, 2008), and in 2015 it reached a staggering 87% nationwide with 86% of homes built since 2000 having a central air conditioning unit (EIA, 2018).

Today, the United States uses the most electricity on air conditioning followed by China (Shah, 2019), but this tendency is expected to grow worldwide. Isaac and van Vuuren (2008) concluded in their study that the global energy demand for air conditioning due to climate change could increase by around 70%, and the demand for heating decrease by more than 30%, augmenting the overall energy demand and creating dangerous peak use moments. Such needs present numerous challenges and therefore significant technological improvements, policy changes, and social initiatives are needed today for a better tomorrow (Santamouris, 2016).

Thermal Comfort

Thermal comfort can be defined as a condition of mind expressing satisfaction with the thermal environment in which a person does not prefer to be warmer or cooler (Vanos, Warland, Gillespie, & Kenny, 2010). Holopainen et al. (2013) explain how human thermal sensation is affected by external parameters such as air temperature, air velocity, and humidity, but also by internal parameters such as metabolic rate, activity level, and clothing. Today´s regulations and expectations dictate certain levels of comfort in parameters such as air temperature, air velocity, and humidity, however, more flexible temperatures could result in better occupant satisfaction and more sustainable practices (Holopainen, et al., 2013; de Dear & Brager, 2002). Therefore, it is pertinent to question and challenge the current comfort parameters dictated by regulation. Considering a wider and more flexible range of thermal comfort parameters integrated with passive design strategies could help improve comfort levels while reducing buildings' energy loads for heating and cooling.

These ranges can be analyzed in bioclimatic diagrams which are used to determine thermal comfort levels as they present on a psychrometric chart the combination of temperature and humidity given any specific climatic characteristics (Givoni, 1991). Victor Olgyay developed the most widely used diagram which was adopted by ASHRAE (Manzano-Agugliaro, Montoya, Sabio-Ortega, & García-Cruz, 2015), and based on the same parameters, has been used and developed in different studies. For example, Manzano-Agugliaro et al. (2015) adapted Givoni's diagram (Figure 3) incorporating the different climatic zones for which it is necessary to use strategies to reach thermal comfort levels, providing guidelines to different passive design strategies. This tool can facilitate the analysis of the climatic conditions of a given location following thermal comfort and guide a building's design so it´s better adapted to its environment, and therefore can be used to guide passive design strategies.

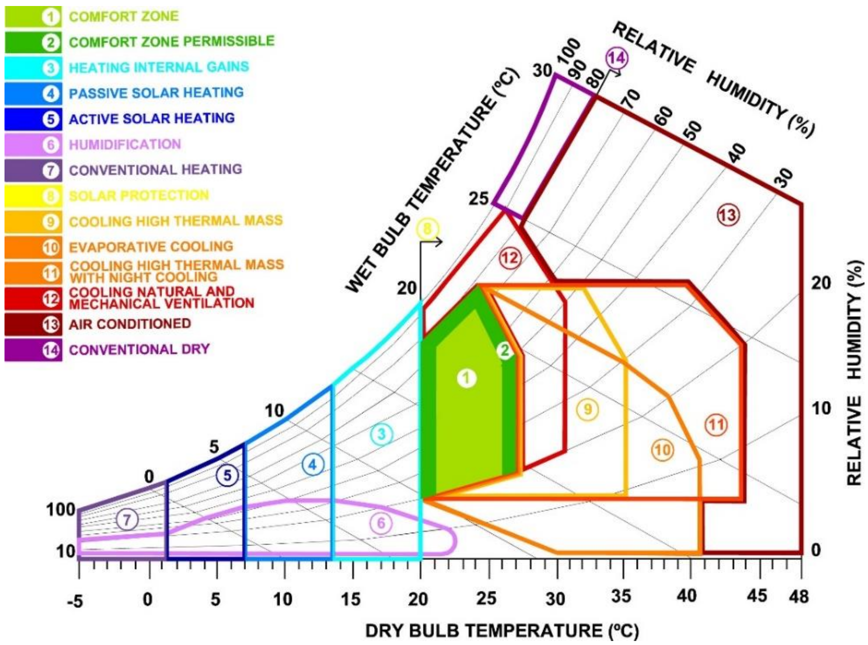

Figure 3: Psychrometric chart (Manzano-Agugliaro, Montoya, Sabio-Ortega, & García-Cruz, 2015)

Bioclimatic Principles

Protecting people from the exterior environment has been inherent to architecture from its origin intending to achieve the best thermal comfort levels which have gradually evolved from a quest for increased comfort to a quest for constant conditions. The concept of bioclimatic architecture is commonly defined as a practice of building design that seeks to achieve human thermal comfort while optimizing energy use by accounting for, and interacting with local climatic conditions, and does it by actively operating on the form and material composition rather than by adding active technologies (Košir, 2019; Manzano-Agugliaro, Montoya, Sabio-Ortega, & García-Cruz, 2015). Similarly, Passive Solar

Architecture refers to design strategies that aim at using on-site solar energy to attain favorable thermal conditions in buildings without the use of mechanical systems (Košir, 2019). These are not contemporary concepts, and architecture has evolved around them throughout history and many examples can be found in vernacular architecture. Since the Industrial Revolution, the application of such passive systems have lost importance as comfort in modern architecture relies on electro-mechanical systems that continuously use energy, however, the current need to reduce buildings' ecological footprint has made bioclimatic design a subject of scientific research and application (Košir, 2019). The use of passive design strategies can help reduce buildings' energy loads particularly for cooling and heating and reducing CO2 emissions (Manzano-Agugliaro, Montoya, Sabio-Ortega, & García-Cruz, 2015). Studies done by Agrawal (1989) determined 2.35% of the world's energy outputs could be saved through proper passive solar design concepts.

Now, every building is characterized by a unique set of conditions, including the topography, orientation, climatic and environmental conditions, mass, volume, and building size, local standards, and materials availability, all of which bioclimatic structures need to consider, eliminating the possibility of applying general rules (Tzikopoulos, Karatza, & Paravantis, 2004). Vernacular architecture and different passive design strategies and solutions can serve as sources of inspiration, and help identify the appropriate measures to be implemented in combination with current technology to achieve climate-adapted buildings (Košir, 2019).

Passive design involves methods of collecting, storing, distributing, and controlling the thermal energy flow through a building´s design, materials, construction methods, and operation practices (Agrawal, 1989). Bioclimatic structures seek to minimize the exposure to cold temperatures and maximize solar gains during the winter months, and minimize the exposure to hot temperatures through various cooling techniques and reduce solar gain during the summer months (Tzikopoulos, Karatza, & Paravantis, 2004). There are different strategies for passive heating and passive cooling and a combination of both can be applied according to the specific characteristics of a building and its location to achieve the most benefits in regards to thermal comfort and energy savings. The greatest opportunity for the integration of passive design strategies starts at the conceptual design level (Pacheco, Ordóñez, & Martínez, 2012), as they relate to many aspects of the building, from its orientation and form to its window-to-wall ratio, materials, glazing type, and insulation to name a few.

Finally, the fundamental objective of passive solar heating is to favor the accumulation of solar radiation within a space and to have a solar absorption strategy to maintain it (Stevanović, 2013), whereas passive cooling as defined by Pacheco et al. (2012) is the means of naturally expelling heat from a space. The proper use of glazing, particularly in the south-facing façade and the application of thermal mass are widely used strategies for passive heating, and natural ventilation, which is discussed below, radiant cooling, and evaporative cooling are widely used passive cooling systems.

Natural Ventilation

Natural ventilation is a design strategy that has been used for centuries around the world to regulate temperatures in buildings and is amongst the most common types of passive cooling strategies. Air movement is the main requirement in the ventilation process and is driven by the buoyancy effect which controls airflow rates due to air temperature and density differences at the inlets and outlets (Chan, Riffat, & Zhu, 2009). Now, the efficiency of natural ventilation is incredibly hard to understand and design as it depends on many factors such as a building’s type, geometry, layout, window-to-wall ratio, window size and location, orientation, and climate, all of which have been studied and documented around the world (Aflaki, Mahyuddin, Mahmoud, & Baharum, 2015; Chen, Tong, & Malkawi, 2017; Izadyar, Miller, Rismanchi, & Garcia-Hansen, 2019). Additionally, avoiding heat and managing to reduce a building's heat absorption from its surrounding environment through better design can significantly improve the cooling potentials of natural ventilation (Aflaki, Mahyuddin, Mahmoud, & Baharum, 2015). To this effect, many mitigation strategies to reduce UHIs have been developed and researched around the world.

As mentioned before, air velocity is one of the main factors determining people´s thermal comfort. At high temperatures, air movement can improve people´s thermal perception, however, elevated air velocity may cause draught discomfort, and deteriorate thermal comfort at lower temperatures (Melikov & Kaczmarczyk, 2012). Therefore, to create comfortable thermal conditions through the use of natural ventilation, adequate air velocity, relative humidity, and air temperature parameters are needed. The current building practice is to avoid higher air velocities as it can be a possible source of draft discomfort. ASHRAE and ISO standards, for example, suggest using in rooms with an air temperature above 26° Celsius (79° Fahrenheit) a maximum air velocity of 0.82 m/s (as cited in Melikov & Kaczmarczyk, 2012). However, recent studies show a preference towards higher rather than lower air movement (Veselý & Zeiler, 2014), particularly when personal control is available (de Dear & Brager, 2002). In fact, with the use of personalized ventilation, it has been shown that thermal comfort can be maintained in rooms with air temperature reaching 30° Celsius (86° Fahrenheit) with a relative humidity of 60% to 70% (Veselý & Zeiler, 2014), widening the possibility for naturally ventilating spaces and further stressing the need to challenge current comfort parameters.

Now, many passive design strategies have been developed but they generally have some limitations (Chan, Riffat, & Zhu, 2009), and as previously mentioned, maintaining a tolerable indoor air temperature in overpopulated cities can be difficult. However, recent studies have shown positive results for hybrid ventilated buildings coupling natural ventilation with mechanical ventilation (Chen, Augenbroe, & Song, 2018; Ezzeldin & Rees, 2013). A review of buildings having a mixed-mode ventilation system done by Salcido et al. (2016) found that buildings with a mixed-mode ventilation system have the potential to save 40% of energy-related to the HVAC system by optimizing window operation schedules, and up to 75% by alternating natural and mechanical ventilation. Therefore, there are many different ways and set of strategies that can help reduce the energy load of buildings.

Buildings´ climate adaptability has not always been prioritized in architecture today because of technological advances and the introduction of air conditioning. However, studies have shown that natural ventilation can reduce energy consumption and greenhouse gas emissions, increase both the degree of indoor and outdoor thermal comfort, and significantly improve air quality (Aflaki, Mahyuddin, Mahmoud, & Baharum, 2015), all contributing to a healthier and more sustainable environment. The requirements for summer cooling and winter heating may indeed be continuous, but, day-to-day variations make it difficult for bioclimatic architecture to maintain thermal comfort throughout the year. Nevertheless, applying passive strategies in combination with electro-mechanical systems can still help reduce the energy demand and have a positive impact on buildings´ footprint. Passive design strategies should always be considered and implemented in designs and even if they are insufficient at eliminating a building´s energy consumption, they can still offer a pathway to less energy-intensive constructions.

Chapter 3: Study Area

This chapter introduces the case study location I have chosen (Austin, Texas) to evaluating the cooling potential of green facades to reduce UHIs, improve thermal comfort, increase the potential of natural ventilation, and reduce building´s cooling loads. The chapter also presents and justifies the specific case study site chosen for running simulations.

ABOUT AUSTIN, TEXAS

Austin is the capital city of the State of Texas and is located within Travis County. It is the eleventh most populous city in the United States with a total population of 978,908 and is one of the fastest-growing large cities in the country with a 21% population increase since 2010 (U. S. Census Bureau, 2019; U.S. Census Bureau, 2020). With rapid population growth comes a rapid rate of development and a great responsibility to analyze its impacts coupled with a great opportunity to propose innovating solutions to mitigate these impacts.

Austin is located in Central Texas at the junction of the Colorado River and the Balcones Escarpment separating the Texas Hill Country from the prairies to the east (NOAA, n.d.). The elevation of the City varies from 130 meters (425 feet) to over 305 meters (1,000 feet) above sea level, with mainly flat areas with lower elevations to the east and rolling hills with higher elevations to the west (Yamazaki, et al., 2017). Because of these variations in topography, weather conditions can differ between different sectors of the city.

Austin belongs to the Humid Subtropical Climate under the Köppen Climate Classification which is characterized by long, hot, and humid summers and short, mild winters, with warm spring and fall transitional periods (NOAA, n.d.), and under the ASHRAE classification, Austin falls under the climate type “2A”, with the number of cooling days surpassing the number of heating days (EnergyPlus, n.d.). Summers in Austin are long and hot, with an average temperature of 28° Celsius (82.4° Fahrenheit), with normal lows around 24° Celsius (75.2° Fahrenheit), and normal highs above 32° Celsius (90° Fahrenheit) with maximum temperatures reaching 39° Celsius (102.2° Fahrenheit) in August (NOAA, n.d.; EnergyPlus, n.d.). Winters are typically characterized by relatively mild temperatures with the average nearing 13° Celsius (55.4° Fahrenheit), with normal highs around 25° Celsius (77° Fahrenheit) and normal lows around 4° Celsius (40° Fahrenheit) with minimum temperatures reaching -8° Celsius (46.4° Fahrenheit) in January (NOAA, n.d.; EnergyPlus, n.d.). The average temperatures in autumn and spring are 15° Celsius (59° Fahrenheit) and 24°C (75.2° Fahrenheit) respectively (EnergyPlus, n.d.). The elevated levels of humidity, with annual averages ranging from 59% registered in August to 75% registered in May, impact the human thermal perception increasing the temperature in the summer and decreasing it in the winter.

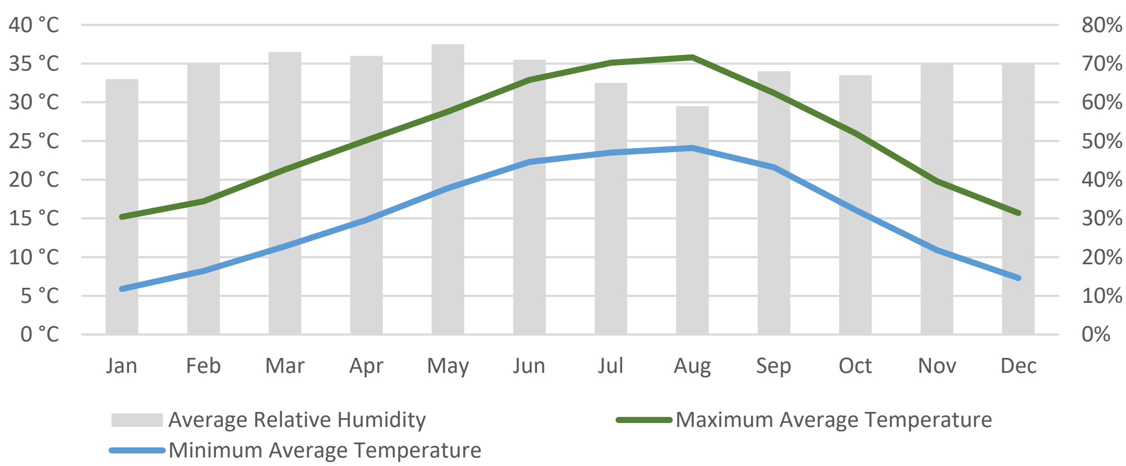

Figure 4: Monthly Average Minimum and Maximum Temperature and Average Relative Humidity Over the Year in Austin. (Data from Weather Atlas, n.d.)

Precipitation in Austin is relatively moderate throughout the year with the heaviest amounts occurring in May and October, in that order, and the least amount of rainfall registering in February. The average annual precipitation levels range from 81 centimeters to 91 centimeters (32 inches to 36 inches), with historical extremes varying from 29 centimeters to 164 centimeters (11.42 inches to 64.68 inches) (NOAA, n.d.; Ward N. , 2009).

Austin is located at a latitude of 30°N allowing for an average of over 12 hours of daylight. The average amount of sunshine varies from 50% in the winter to 75% in the summer as typically Austin does not have a dense cloud cover persisting throughout the day (NOAA, n.d.). As a result, Austin has a significant amount of daylight hours ranging from 10 to 14 hours and sun hours ranging from 5 to 10 hours throughout the year as seen in Figure 5.

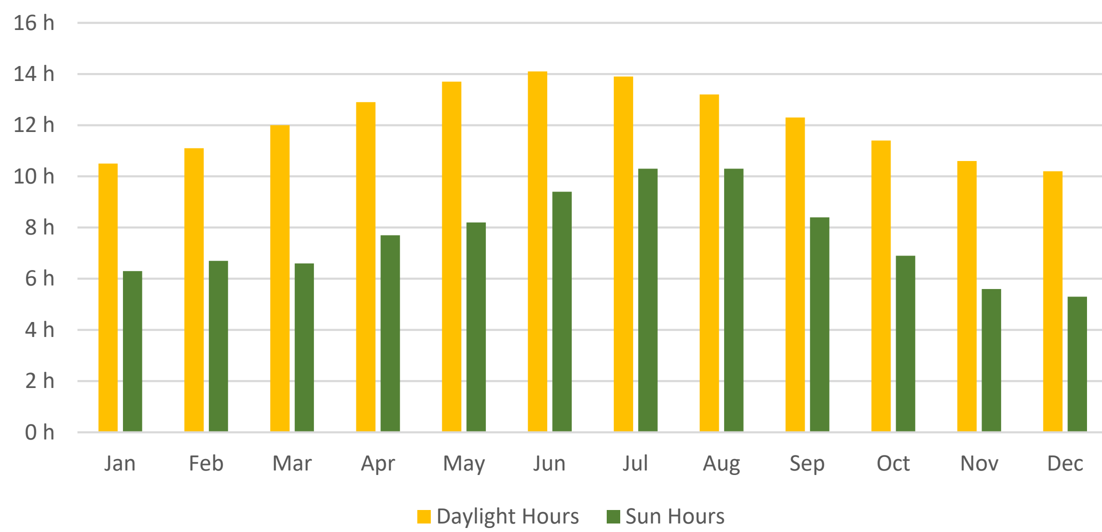

Figure 5: Monthly Average Daylight Hours and Sun Hours Over the Year in Austin. (Data from Weather Atlas, n.d.)

Prevailing winds come typically from the south with some variety to the east, and in the winter occasionally from the north with passing cold fronts. The average annual wind speed is 3.96 meters per second, with the majority of the winds ranging from 3.6 to 5.1 meters per second, and rarely surpassing 10.8 meters per second (Ward N. , 2009).

Severe weather in the form of hail and strong winds impact Austin particularly in March through May (NOAA, n.d.), and extremely high temperatures are reached during the summer months. Tornadoes are uncommon, and tropical storms rarely impact the Austin region but can cause heavy rain resulting in flooding, and Austin is located in a regions know as Flash Flood Alley where devastating flash floods have been registered throughout history (NOAA, n.d.). Generally dryer conditions and elevated winds during the winter months create favorable conditions for Wildfires (NOAA, n.d.).

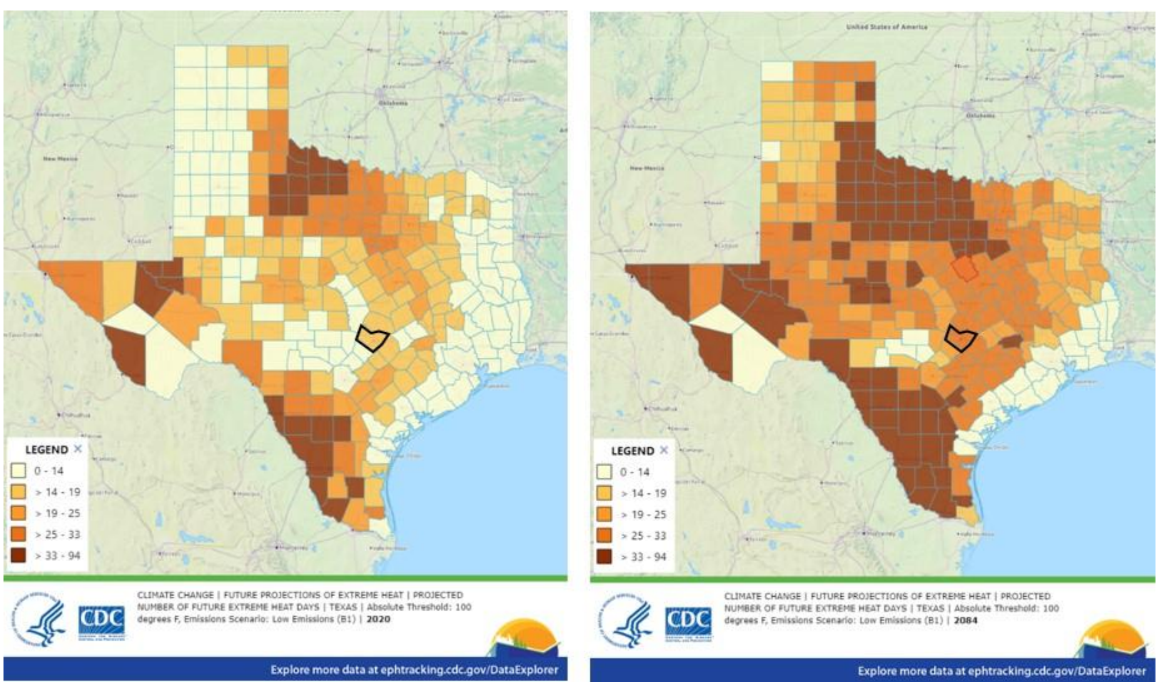

Figure 6: Projected Number of Future Extreme Heat Days in Texas for the Years 2020 and 2084. (CDC, n.d.)

Conclusively, Austin is located in a cooling-dominated climate and the most common climate-related hazards are flood, wildfires, and heat (Bixler & Yang, 2020). With the increasing frequency and intensity of extreme weather events caused by global warming, we must analyze and mitigate our exposure to these events, particularly extreme heat as the Center for Disease Control and Prevention (CDC) projects the number of days of extreme heat with temperatures above 37.8° Celsius (100° Fahrenheit) to increase in Austin due to climate change from 17 days in 2020 to 18 days in 2030, 21 days in 2050 and 29 days in 2084 (CDC, n.d.). Figure 6 shows the projected number of extreme heat days in the state of Texas for the years 2020 and 2084.

CASE STUDY SITE SELECTION

The selection of the case study location was based on identifying residential neighborhoods most vulnerable to heat through a multi-risk climate vulnerability assessment for Austin developed by Bixler and Yang (2020) and current land-use zoning (CodeNEXT, 2018). Using publicly available data and linking vulnerability, hazard risk, and resilience, Bixler and Yang (2020) created a tool to identify specific neighborhoods (spatially designed as census block groups) with exposure to one or multiple hazards coupled with high social vulnerability. They developed indices for the three most common hazard risks in Austin independently (flood, wildfire, and heat), and quantified social vulnerability considering populations with characteristics associated with high sensitivity and a low ability to adapt, respond, and bounce forward. They calculated the urban heat hazard exposure using imperviousness as the primary indicator and tree cover. Figure 7 shows their result for the heat hazard risk highlighting in red the most vulnerable neighborhoods with an index score of 0.5 to 1 (on a 0 to 1 scale).

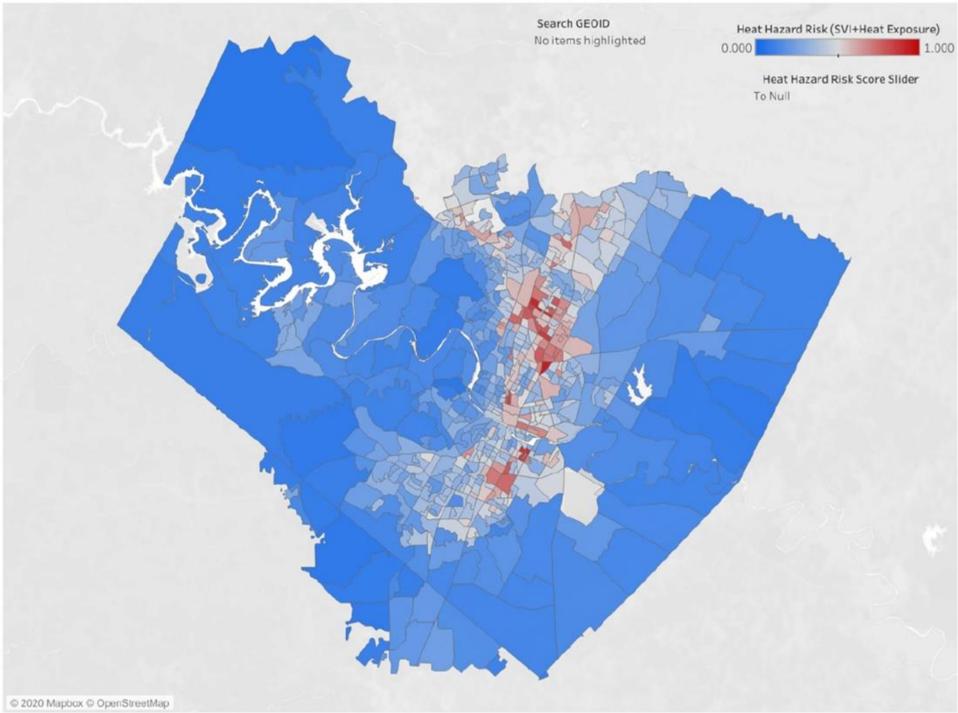

Figure 7: Austin Heat Risk (hazard exposure & vulnerability) by Bixler and Yang (2020).

Identifying the most vulnerable neighborhoods with an index score of 0.6 to 1 in Bixler and Yang's analysis, and isolating the areas with prevailing zoning categorized as Single Family Residence extracted from (CodeNEXT, 2018), 26 census groups were identified (shown in Figure 8). To determine the final case study site, the 26 neighborhoods' mean population and mean number of residential units were calculated resulting in 1,868 and 654 respectively. Finally, these findings lead to the selection of a representative neighborhood identified as census block group 484530009023.

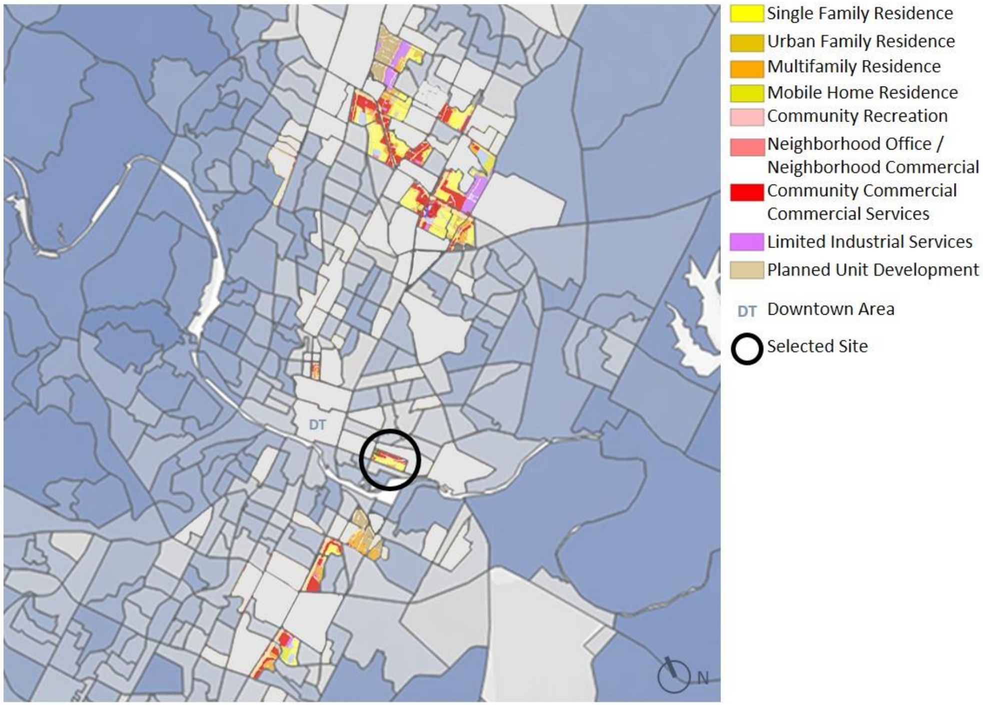

Figure 8: Austin heat risk vulnerable neighborhoods and current zoning (adapted from Bixler & Yang, 2020 and information extracted from Census Block Group Map, 2020).

CASE STUDY LOCATION

The selected neighborhood is identified as census block group 484530009023 and has a population of 1,566 and 577 residential units (Census Block Group Map, 2020). It is located close to the downtown area, at about 1.6 km (1 mile), and is bordered by E. Cesar Chavez Street to the south, Chicon Street to the west, E. 5th Street to the north, and Pleasant Valley Road N. to the east. Single-family residential is the predominant land use, followed by neighborhood office and neighborhood commercial located primarily along E. Cesar Chavez Street, and limited industrial services on E. 5th Street.

The specific case study site to be modeled and analyzed is located on the west end of the selected neighborhood. The area is delimited by Robert Martinez Jr. Street to the east while the other boundaries remained unchanged. In this area can be found several different land uses including single-family residential, commercial, and industrial (CodeNEXT, 2018). In general terms, the north-most end is categorized by commercial and industrial buildings, followed to the south by a neighborhood park (Pan American Neighborhood Park) and a school (Zavala Elementary School), then residential houses, and finally office and commercial buildings along E. Cesar Chavez Street.

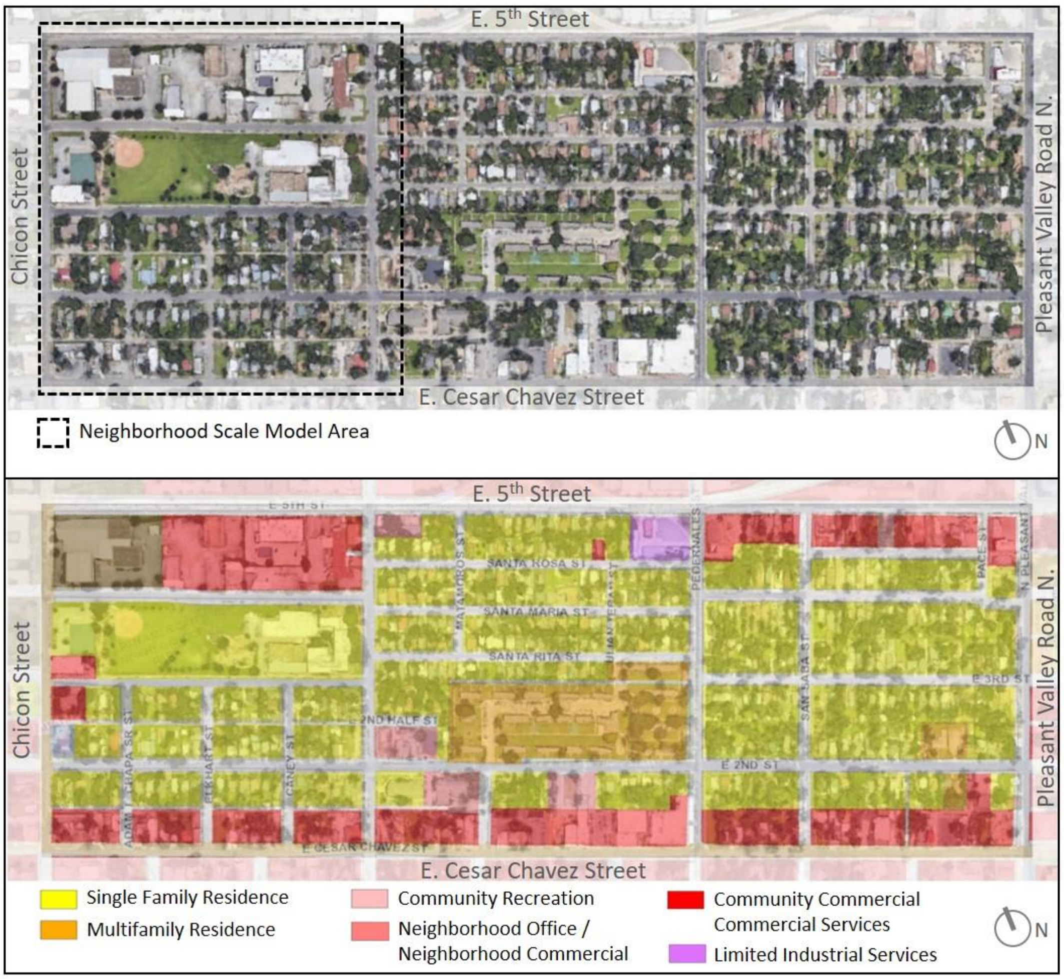

Figure 9: Screenshot of the selected neighborhood highlighting the neighborhood scale model area and indicating the current zoning (Image from Google Maps, 2020, adapted with data extracted from Census Block Group Map, 2020).

Chapter 4: Methodology

This chapter introduces the software used to model and run simulations. A brief overview of the ENVI-met software is presented followed by a description of the parameters and settings used in the two models created for this analysis.

ENVI-MET SOFTWARE

Numerical methods to analyze urban microclimate are essential tools for engineers, architects, urban planners, and policymakers to compare urban design alternatives, determine best practices, and establish guidelines (Toparlar, Blocken, Maiheu, & Heijst, 2017). With ENVI-met software, one of the most widely used dynamic simulation tools for microclimate analysis (Tsoka, Tsikaloudaki, & Theodosiou, 2018), it is possible to analyze a design's impact on the local environment which can help mitigate factors such as heat stress, air pollution, or wind risk.

ENVI-met is a three-dimensional, grid-based, microclimate model used to simulate complex urban environments as holistic organisms. The model is based on the fundamental laws of fluid dynamics and thermodynamics and can simulate the dynamic interactions between plants, buildings, and the atmosphere on a microscale level with a typical spatial resolution ranging between 0.5 to 10 meters and time steps of 1 to 10 seconds (Huttner, 2012). This enables the capacity to analyze a wide range of spatial scales from a small courtyard to entire cities. The main variables ENVI-met calculates, using several sub-model shown in Figure 10, are air temperature, surface temperature, relative humidity, wind speed and direction, turbulence, radiative fluxes, and air pollutant dispersions (Huttner, 2012). The model´s detailed characteristics, structure, and mathematical equations are provided in (Bruse & Fleer, 1998; Huttner, 2012).

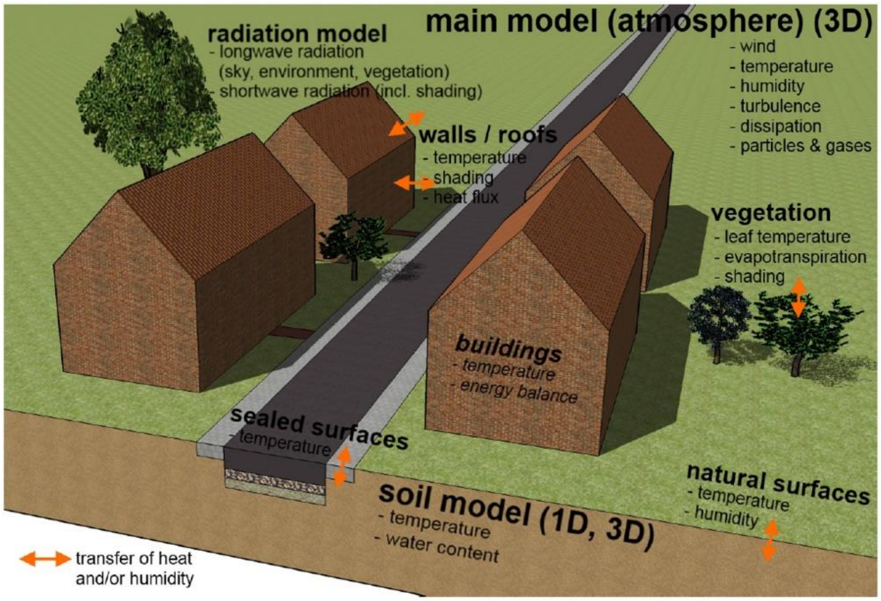

Figure 10: Schematic of the sub-models of ENVI-met (Huttner, 2012).

Professor Michael Bruse started the model´s design in 1994 and has continued developing it ever since with his team at the University of Mainz (ENVI-met, 2021). The first official version of ENVI-met (version v3) was released in 1998 followed by version v4 released in 2014 to which additional features and smaller updates were added giving way to the current version: v4.4.5 summer20 (ENVI-met, 2021). The main differences between the versions v3 and v4 are that the newer version provides a new forcing system of air temperature and relative humidity input parameters resulting in higher simulation accuracy, it is now able to simulate shading objects independent of the building structures, fountains, and water spray-type systems, allows the user to add thermal mass and heat inertia on the building elements, and the incorporation of a 3D vegetation model allowing users to simulate and create complex vegetation geometries (Tsoka, Tsikaloudaki, & Theodosiou, 2018). In version v4.4, a greening module that allows simulating the effects green walls and green roofs have on the energy performance of buildings and their impacts on the outdoor climate was added (Peng, et al., 2020).

Plants are integrated into the model as living organisms interacting with the surrounding environment by heat abortion and evapotranspiration (Peng, et al., 2020; Morakinyo, Lai, Lau, & Ng, 2019). The latest additions relating to plants allow to create and manage the vegetation´s properties and appearance and enable the creation of new plants accounting for the root shape, canopy size, leaf area index (LAI), leaf albedo, and the ability to distinguish between evergreen and deciduous species. The new greening module allows greenery systems to be placed directly on building facades and roofs, and define the properties of the vegetation and the substrate layer located between the plant and the building's surface.

A review by Tzoka et al. (2018) found the number of publications using the ENVI-met model significantly augmented since 2011, with most of the studies having been conducted in Europe and Asia in that order, and performed in areas characterized by humid subtropical climate. In their study, the authors explain the vast majority of the studies only evaluated the model´s performance during the summer months, and, unlike the parameter of wind which was rarely used for evaluating the model, air temperature was the most widely evaluated microclimatic variable. Finally, they found that adding greenery was the most commonly investigated mitigation strategy with the majority of the studies focusing on the cooling potentials of street trees and green roofs and focusing much less on green walls or the combination of various strategies.

SIMULATION MODELS

For this study, two different-scale models were created in ENVI-met to better understand the effects direct green facades have on the air temperature, surface temperature, and relative humidity at a neighborhood and a single building scale. In both cases, I ran several simulations considering different green facade quantities and locations and simulated a baseline model to measure and compare the impacts of these strategies. All the models were set to run for 24 hours starting at 7 am on July 18, 2018, with simple forcing boundary conditions using self-defined minimum and maximum air temperatures (25°C to 39°C), and wind speed and direction (2.5 m/s winds coming from the south). ENVI-met default soil, building materials, and vegetation listed in Table 1 were used in all models.

Buildings			
	Wall	Default Wall - Moderate insulation	
	Roof	Default Wall - Moderate insulation	
	Windows	Heat Protection Glass (one Layered)	G1
	Facade Greening	Only green	1NAFG
Soil and Surfaces			
	Natural Surfaces	Loamy Soil	
	Roads and Pavements	Asphalt Road	ST
		Concrete Pavement Gray	PG
		Concrete Pavement Light	PL
		Pavement (Concrete), used/dirty	PP
Vegetation			
	Simple Plants	Grass 25cm aver. Dense	XX
		Ivy (Hedera helix)	IV
		Tree 10 m very dense, leafless base	T1
		Tree 20 m very dense, distinct crown	SM
	3D Plants	Decidious Tree	DM

Table 1: Key input parameters for ENVI-met modeling.

Neighborhood scale model

The model dimensions were 100 x 100 x 25 grids (x, y, z) covering the previously described neighborhood section. A special resolution of 5m x 5m (dx, dy) and 2m height (dz) was used. One intervention and a reference baseline scenario were generated. The intervention model consisted of adding a direct green façade on every building and every orientation. It is important to note that while adding a direct green façade on every building and every orientation is unrealistic, the purpose of this model is to investigate the maximum impact direct green facades have on the air temperature, surface temperature, and relative humidity at a neighborhood scale. All other main parameters were left unchanged to only evaluate the effects of the described case on the urban environment. Key input parameters and data acquisition information are given in Table 1 and Table 2. The model´s plan configuration and layout can be seen in Figure 11 along with the 3D view of the model.

Model Domain Settings						
Model dimensions	x	100	y	100	z	25
Size of grid cell (meters)	dx =	5.00	dy =	5.00	dz =	2.00 (base)
Methods of vertical grid generation	dz of lowest gridbox is split into 1% telescoping factor after				5 subcells 17m height	
Model rotation out of grid north	20°					
Model Geometry Overview						
Core xy domain size (meters)	X:	500	Y:	500		
Height of 3D model top	52.86 meters					
Highest point building	11.00 meters					

Table 2: Neighborhood scale model domain settings and geometry overview.

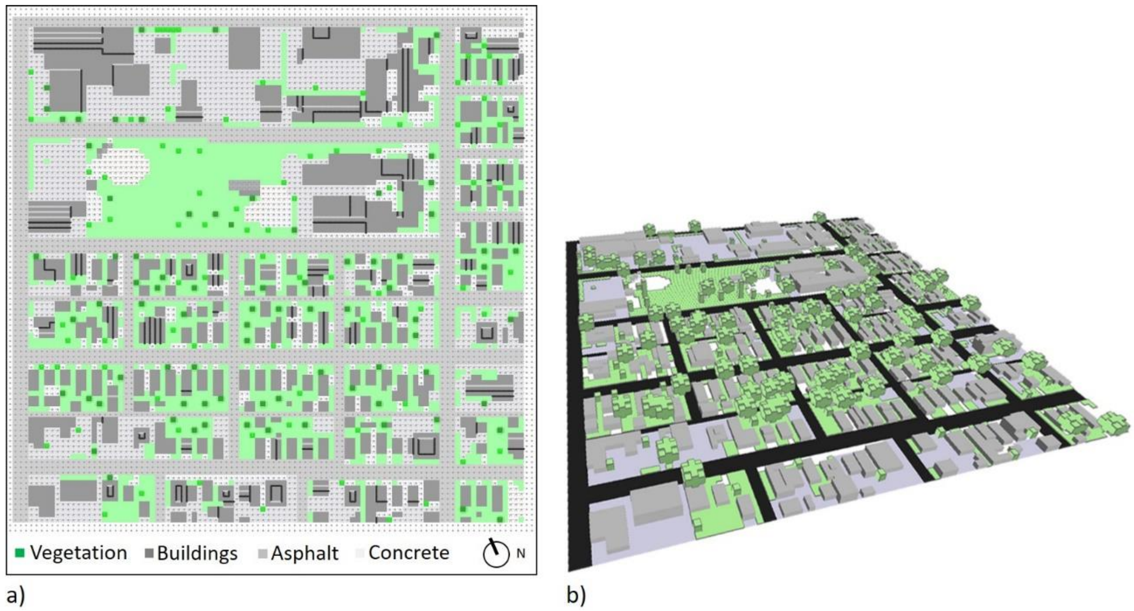

Figure 11: Neighborhood scale model a) plan view, and b) 3D view.

Building scale model

The model dimensions were 45 x 80 x 30 grids (x, y, z) covering a typical single-family house found in the selected neighborhood, a section of the adjacent houses, and surrounding streets. A fin special resolution of 1m x 1m (dx, dy) and 1m height (dz) was used. Three interventions and a reference baseline scenario were generated. The intervention models consisted of adding a direct green façade on every wall of the main building and the surrounding border wall at different heights. In the first intervention (GW_1m), a 1-meter tall green façade was proposed on all walls, in the second intervention (GW_2m) a 2-meter tall green façade was proposed, and finally, and in the third intervention (GW_4m) a 4-meter tall green façade covering the entire wall height was proposed. The only places greenery was not added in all scenarios were the covered front and back porches. All other main parameters were left unchanged to only evaluate the effects of the described cases on the urban environment. Key input parameters and data acquisition information are given in Table 1 and Table 3. The model´s plan configuration and layout can be seen in Figure 12 along with the 3D view of the model.

Model Domain Settings						
Model dimensions	x	45	y	80	z	30
Size of grid cell (meters)	dx =	1.00	dy =	1.00	dz =	1.00 (base)
Methods of vertical grid generation	dz of lowest gridbox is split into 5% telescoping factor after				5 subcells 16m height	
Model rotation out of grid north	20°					
Model Geometry Overview						
Core xy domain size (meters)	X:	45	Y:	80		
Height of 3D model top	36.58 meters					
Highest point building	6.00 meters					
Building wall top height	4.00 meters					
Boarder wall top height	2.00 meters					

Table 3: Building scale model domain settings and geometry overview.

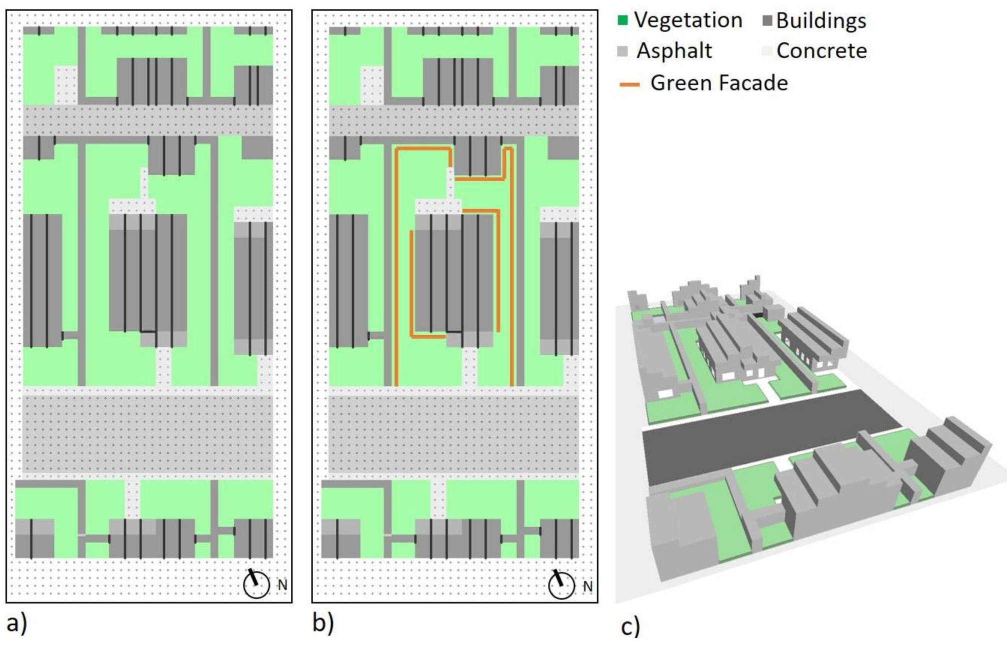

Figure 12: a) Building scale site plan model; b) Site plan depicting the walls with added greenery; c) Building scale 3D view.

Chapter 5: Findings

In the following chapter, the atmospheric temperature and relative humidity for the different models and scenarios are presented and discussed. The results are shown for the neighborhood scale and the building scale independently. The measurements are analyzed at a pedestrian height, representing what people would be able to perceive, and at a one-floor-building height to better understand the impacts green walls have on the building facades. To appreciate the temperature oscillations simulated by the software, and to compare modeled air temperatures on specific areas and the surface temperatures on specific facades, several points are identified throughout the area of each model.

Neighborhood scale model

For the neighborhood scale model, the measurements are analyzed at a pedestrian height of 1.40 m, and a building height of 3.00 m. To better understand the temperature oscillations simulated by the software in both the air temperature and surface temperature, 18 points were identified throughout the area. The location of these receptors is shown in Figure 13. Table 4 shows the maximum temperature difference between the proposed scenario and the baseline model for the overall minimum and maximum potential air temperatures, the wall temperatures, and the zone temperatures.

The overall simulated potential atmospheric relative humidity barely increased from 8 am to 10 pm when greenery was added, registering a maximum difference at a pedestrian height from 59.89% to 61.03% at noon, and a building height of 3.00 m from 55.39% to 56.35% at 6 pm. The overall minimum and maximum potential air temperature differences were strongest at 6 pm registering a cooling effect of up to 0.19°C, however, the overall minimum and maximum potential air temperature differences also show an increase of up to 0.17°C registered at 7 am.

Figure 13: a) Site plan depicting the position of the receptors on the ground; b) Site plan depicting the position of the receptors on the facades.

Minimum Overall Potential Air Temperature Difference °C)				Maximum Overall Potential Air Temperature Difference °C)				
At 1.40m -0.14		At 3.00m -0.17			At 1.40m 0.18		At 3.00m 0.19	
	Zone Air Temperature Difference °C)			Maximum Wall Temperature Difference °C)				
		At 1.40m			At 1.40m		At 3.00m	
		Min.	Max.		Min.	Max.	Min.	Max.
South	R1	-0.07	0.12	F1	-0.19	4.09	-0.24	4.11
South	R5	-0.09	0.12	F5	-0.12	4.22	-0.17	4.24
South	R9	-0.07	0.11	F9	-0.13	4.02	-0.21	4.11
South	R13	-0.10	0.14	F13	-0.19	4.19	-0.23	4.22
West	R2	-0.11	0.23	F2	-0.25	4.86	-0.28	4.92
West	R8	-0.19	0.23	F8	-0.04	5.10	-0.06	5.21
West	R10	-0.08	0.17	F10	-0.35	4.78	-0.41	4.82
West	R14	-0.13	0.21	F14	-0.41	4.83	-0.45	4.80
West	R17	-0.11	0.21	F17	-0.34	4.75	-0.37	4.72
West	R18	-0.12	0.17	F18	-0.30	4.78	-0.41	4.79
North	R3	-0.16	0.16	F3	0.34	2.99	0.30	3.21
North	R11	-0.20	0.19	F11	0.31	2.38	0.30	2.26
North	R15	-0.19	0.15	F15	-0.68	1.75	-0.79	1.65
North	R7	-0.14	0.12	F7	-0.34	3.61	-0.17	3.67
East	R4	-0.07	0.13	F4	-0.40	4.90	-0.42	4.95
East	R6	-0.12	0.16	F6	-0.39	4.87	-0.50	4.87
East	R12	-0.08	0.10	F12	-0.36	4.75	-0.40	4.64
East	R16	-0.07	0.11	F16	-0.50	4.80	-0.55	4.79

Table 4: Maximum difference between the proposed scenario and the baseline model for the overall air temperature, the wall temperature, and the zone temperature.

Similar to the overall minimum and maximum temperatures, the specific receptors located at a pedestrian height of 1.40m show a temperature reduction between 4 pm and 8 pm of up to 0.23°C registered at 6 pm for R2 and R8. However, they also present a temperature increase reaching the highest point early in the morning registering a temperature increase of up to 0.20°C at 8 am for R11. Thermal maps of the analyzed area are shown in Figure 14, depicting the potential air temperature at 8 am and 6 pm at a pedestrian height of 1.40m.

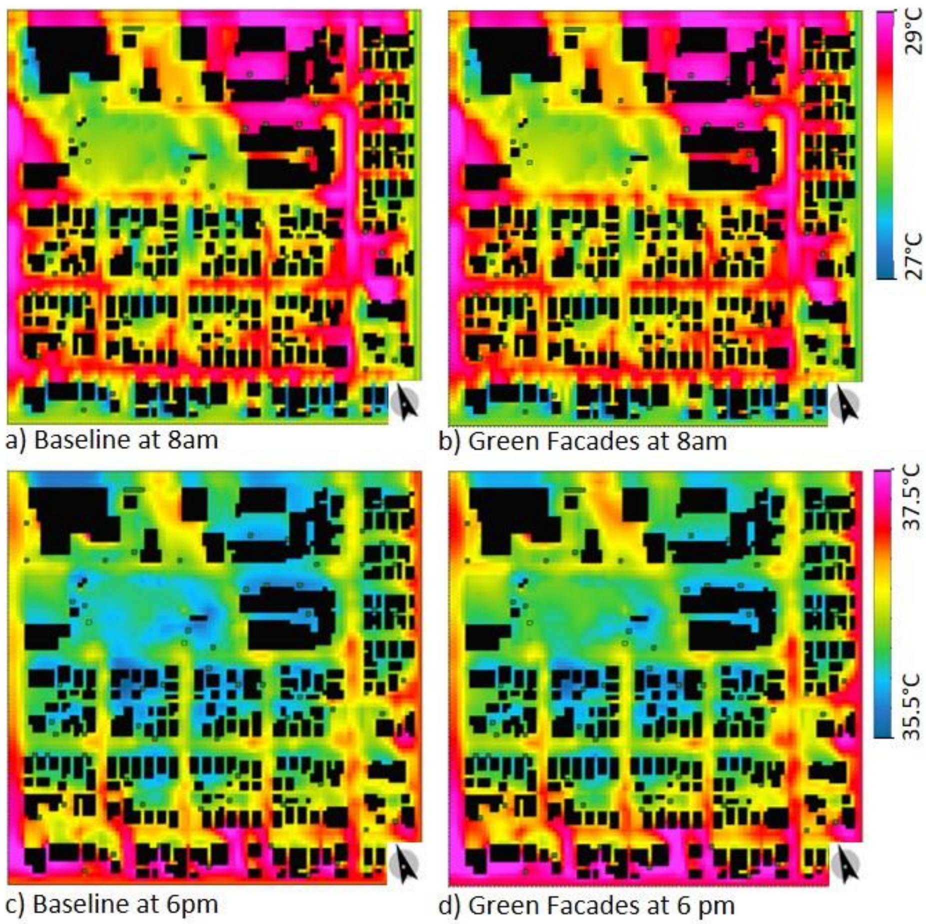

Figure 14: Potential air temperature x-y views at z = 1.40m in a) baseline at 8 am, b) green facades at 8 am, c) baseline at 6 pm, and d) green facades at 6 pm.

The added green walls impacted all the analyzed facades similarly showing maximum wall temperature reductions between 4.02°C and 5.21°C in the south, east, and west facades, and up to 3.61°C in the north façade. The highest differences were registered between 12 pm and 5 pm except for the north-facing façades at R3, and R7, and the east-facing façade at R12 which registered their maximum difference at 10 am. The green walls also slightly increased the wall temperatures from 1 am to 7 am, showing a maximum wall temperature increase of 0.68°C at a pedestrian height, and 0.79°C at the building height, in both cases at R15, a north-facing facade.

Conclusively, adding green facades barely increased the simulated potential relative humidity, and reduced the simulated overall potential air temperature from 4 pm to 8 pm up to 0.19°C, but increased the air temperature up to 0.17°C registered at 7 am. The simulated potential air temperatures were slightly higher at the pedestrian height (1.40 m) compared to the building height (3.00 m). The specific receptors located at a pedestrian height of 1.40m show maximum temperature reductions between 4 pm and 8 pm registering a temperature reduction up to 0.23°C, but also present a temperature increase reaching the highest point early in the morning registering a temperature increase of up to 0.20°C. Finally, the added greenery mostly impacted the surface temperature showing temperature reductions between 12 pm and 5 pm of up to 5.21°C, but also slightly increased the wall temperatures from 1 am to 7 am, showing a maximum wall temperature increase of 0.68°C.

Building scale model

For the building scale model, the measurements are analyzed at a pedestrian height of 1.50 m, and a building height of 3.50 m. To better understand the temperature oscillations simulated by the software in both the air temperature and surface temperature, six points were identified throughout the area. The location of these receptors is shown in Figure 15. Table 5 shows the maximum temperature difference between the three proposed scenarios and the baseline model for the overall minimum and maximum potential air temperatures, the wall temperatures, and the zone temperatures.

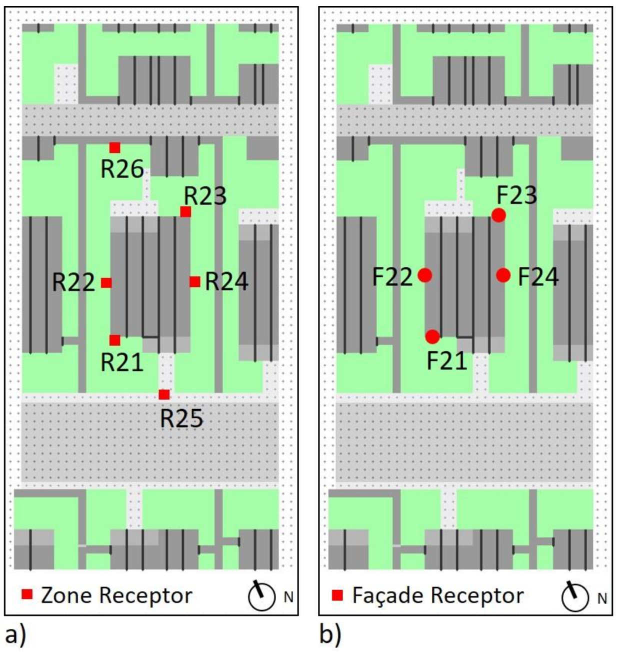

Figure 15: a) Site plan depicting the position of the receptors on the ground; b) Site plan depicting the position of the receptors on the facades.

The model GW_1m did not significantly increase or reduce the simulated minimum and maximum potential air temperature or the simulated potential relative humidity, and the model GW_4m presents the highest temperature and relative humidity modifications. The overall simulated potential atmospheric relative humidity barely increased when greenery was added, registering a maximum difference at a pedestrian height from 56.50% to 57.01% at 1 pm in the model GW_4m, and a building height from 69.29% to 69.61% at 8 am in the same model. The overall minimum and maximum potential air temperature differences were strongest between 4 pm and 9 pm registering a cooling effect of up to 0.09°C registered at 8 pm in GW_4m.

Potential Air Temperature Differnces (°C)							
			Baseline	GW_1m	GW_2m	GW_4m	
Minimum Potential Air Temperature at 1.5m			25.52	25.57	25.51	25.5	
Maximum Potential Air Temperature at 1.5m			39.44	39.44	39.45	39.45	
Minimum Potential Air Temperature at 3.5m			25.74	25.84	25.74	25.73	
Maximum Potential Air Temperature at 3.5m			38.98	38.98	38.98	38.99	
Orientation	Receptor	Minimum difference			Maximum difference		
		GW_1m	GW_2m	GW_4m	GW_1m	GW_2m	GW_4m
South	R21 at 1.5m	-0.01	-0.02	-0.03	0.01	0.04	0.05
West	R22 at 1.5m	-0.02	-0.02	-0.03	0.05	0.13	0.22
North	R23 at 1.5m	-0.02	-0.03	-0.02	0.04	0.11	0.14
East	R24 at 1.5m	-0.01	-0.02	0.00	0.04	0.10	0.13
Front	R25 at 1.5m	0.00	-0.01	-0.01	0.00	0.00	0.00
South_BW	R26 at 1.5m	-0.02	-0.05	-0.06	0.03	0.09	0.12
South	R21 at 3.5m	0.00	-0.01	-0.02	0.01	0.01	0.05
West	R22 at 3.5m	-0.01	-0.01	-0.03	0.02	0.04	0.18
North	R23 at 3.5m	0.00	-0.01	-0.01	0.02	0.05	0.08
East	R24 at 3.5m	0.00	-0.01	0.01	0.01	0.04	0.11
Front	R25 at 3.5m	0.00	0.00	-0.01	0.00	0.00	0.00
South_BW	R26 at 3.5m	-0.01	-0.02	-0.02	0.02	0.05	0.08
Orientation	Receptor	Minimum difference			Maximum difference		
		GW_1m	GW_2m	GW_4m	GW_1m	GW_2m	GW_4m
South	F21 at 1.5m	-0.02	-0.45	-0.45	0.01	4.81	4.76
West	F22 at 1.5m	-0.04	-0.36	-0.36	0.03	4.70	4.64
North	F23 at 1.5m	-0.04	0.07	0.09	0.03	3.22	3.20
East	F24 at 1.5m	-0.04	-0.45	-0.46	0.03	4.63	4.60
South	F21 at 3.5m	-0.02	-0.03	-0.51	0.01	0.02	4.76
West	F22 at 3.5m	-0.05	-0.06	-0.63	0.02	0.04	4.41
North	F23 at 3.5m	-0.04	-0.05	-0.62	0.02	0.03	3.29
East	F24 at 3.5m	-0.04	-0.05	-0.69	0.02	0.04	4.65

Table 5: Maximum difference between the proposed scenarios and the baseline model for the overall air temperature, the wall temperature, and the zone temperature.

Similar to the overall minimum and maximum temperatures, the specific receptors located at a pedestrian height show no significant modifications in model GW_1m, with a maximum air temperature difference of 0.05°C registered at R2 at the pedestrian height. The model GW_2m shows some cooling effects, but the highest differences are presented in model GW_4m. These temperature reductions are highest between 4 pm and 8 pm with the peak registered at 6 pm for R22 (west-facing façade) with a value of 0.22°C at the pedestrian level and 0.18°C at the building height. Thermal maps of the analyzed area are shown in Figure 16, depicting the potential air temperature at 6 pm at a pedestrian height.

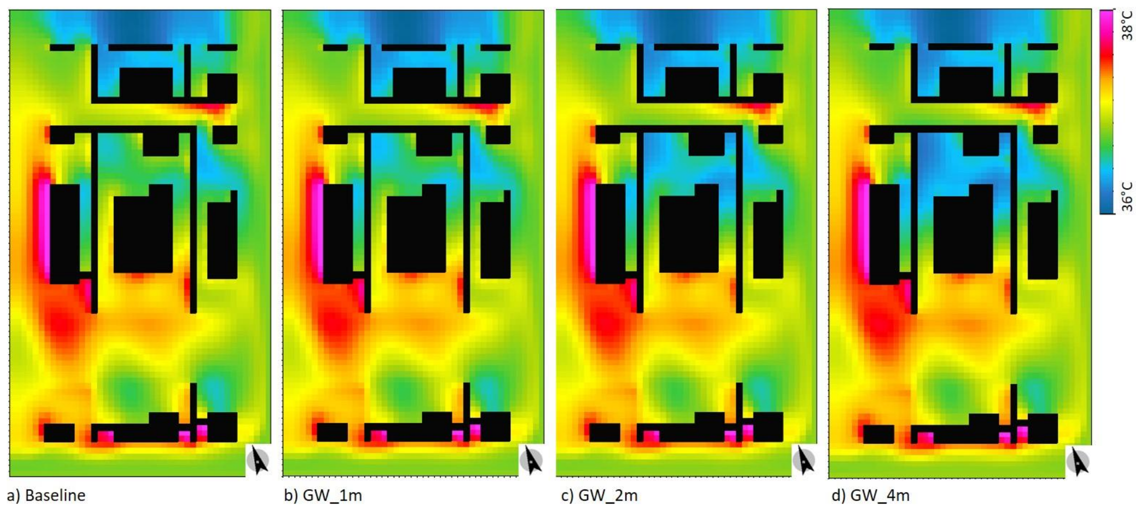

Figure 16: Potential air temperature at 6pm, x-y views at z = 1.50m in a) baseline, b) GW_1m, c) GW_2m, d) GW_4m.

Once again, the added greenery did not significantly modify the surface temperature in model GW_1m. Model GW_2m only shows a surface cooling effect at the pedestrian height, as the walls were not covered with greenery above 2 meters. Both the GW_2m and GW_4m present maximum wall temperature reductions from 8 am to 7 pm with the peak reduction ranging from 3.20°C registered at a building height at R23 at 10 am, to 4.76°C registered at 2 pm at R1 and a pedestrian height. The models also present a slight increase of the surface temperature at night with a maximum temperature increase of 0.69°C registered at 6 am at R24 with a building height.

Chapter 6: Discussion and Conclusions

This research aimed at studying the summer cooling effects of green walls to reduce UHIs, improve thermal comfort, increase the potential of natural ventilation, and reduce buildings' cooling loads. Using ENVI-met model simulations, this study investigated the influence of green facades on the ambient air temperature and its role on the air fluctuations in the hot humid climate of Austin at both a neighborhood and a building scale, with a primary focus on pedestrian height and one-story building average wall height temperature variations.

The results of this research indicate that the added green facades mostly impact the surface temperature. The neighborhood greening resulted in surface temperature reductions during the peak hours of heat between 12 p.m. and 5 p.m. with a maximum cooling effect of 5.21°C, and the building scale greening showed surface temperature reductions during the hours of sunlight from 8 a.m. to 7 p.m. with a maximum cooling effect of 4.76°C registered at the pedestrian height, and 3.20°C at the building wall height. Nevertheless, the added greenery also slightly increased the surface temperature at night with a maximum increase of 0.69°C. Additionally, the simulation results show air temperature reductions between 4 p.m. and 8 p.m. with a maximum cooling effect of 0.23°C. This small air temperature reduction is consistent with previous studies that have reported green facades may not considerably change the air temperature. At the neighborhood scale, a slight air temperature increase at night with a maximum value of 0.20°C was also registered. Finally, the added greenery barely increased the relative humidity, and the air temperature was found to be slightly higher at the pedestrian height compared to the building height.

Conclusively, adding green walls reduces the surface temperature during the peak heat hours when the energy demand is at its highest, which can help reduce the stress imposed on the electrical grid and diminish the likelihood of power outages caused by this demand surplus. Furthermore, the surface temperature reduction indicates the greenery protects the building facades from the heat, reducing a building´s heat absorption which could potentially reduce its cooling loads. Managing to reduce a building's heat absorption from the surrounding environment can significantly improve the cooling potentials of natural ventilation (Aflaki, Mahyuddin, Mahmoud, & Baharum, 2015), which is another design strategy that can help regulate building temperatures, and further reduce energy consumption and improve thermal comfort conditions.

In addition to potentially reducing a building´s cooling loads by protecting its facades from the heat and increasing the potential of natural ventilation, the added greenery can provide many environmental benefits such as reducing greenhouse gas emissions, air and noise pollution (Radic, Dodig, & Auer, 2019), UHI (Andoni & Wonorahardjo, 2018), acidic rain, water runoff (Sedlak, 2014), and improve thermal comfort, human health and well-being (Hartig & Kahn Jr., 2016; Tzoulas, et al., 2007; Elsadek, Liu, & Lian, 2019), and enhance biodiversity (Douglas & James, 2015). Making the benefits of adding greenery to urban areas immeasurable.

Managing to incorporate greenery into overpopulated cities has proven to be challenging, and adding green walls presents several challenges and limitations such as the restricted number of surfaces they are preferably grown. However, the constant rejuvenation of cities allows for architects, engineers, planners, and policymakers to incorporate green walls and other strategies into the design and regulations to create climate-sensitive buildings. As one of the fastest-growing cities in the U.S., Austin has the potential to substantially incorporating these strategies and increase urban vegetation.

This research has several limitations that could be addressed in future studies. First, other mitigation strategies such as adding trees, green roofs, or combinations of these, which previous research has found to provide additional cooling effects, would provide a wider understanding of the possible cooling effects resulting from integrating greenery into the built environment. Second, validating the computer simulation results with field measurements would provide additional scientific evidence of the thermal benefits of façade greening. Third, a more detailed and varied building materials selection would be beneficial for understanding and comparing the cooling potential of different structures. Finally, simulating the building's energy loads using other tools would provide a more holistic analysis and an accurate estimation of the energy effect of façade greening.

References

AAAS. (2009, December 4). *American Association for the Advancement of Science*. Retrieved from www.aaas.org: https://www.aaas.org/news/aaas-reaffirms-statements-climate-change-and-integrity

Ackermann, M. E. (2002). *Cool Comfort: America's Romance with Air-conditioning.* Washington, D.C: Smithsonian Institution Press.

Aflaki, A., Mahyuddin, N., Mahmoud, Z. A.-C., & Baharum, M. R. (2015). A review on natural ventilation applications through building facade components and ventilation openings in tropical climates. *Elsevier: Energy and Buildings 101*, 153-162.

Agrawal, P. C. (1989). A Review of Passive Systems for Natural Heating and Cooling of Buildings. *Solar and Wind Technology Vol. 6, No. 5*, 557-567.

Akbari, H., & Kolokotsa, D. (2016). Three decades of urban heat islands and mitigation technologies research. *Elsevier - Energy and Buildings 133*, 834–842.

Akbari, H., & Rose, L. S. (2007). Urban Surfaces and Heat Island Mitigation Potentials. *Journal of the Human-Environmental System*, Vol. 11; No. 2: 85–101.

Andoni, H., & Wonorahardjo, S. (2018). A Review on Mitigation Technologies for Controlling Urban Heat Island Effect in Housing and Settlement Areas. *IOP Conference Series: Earth and Environmental Science 152 012027.*

Baciu, I. R., Lupu, M. L., & Maxineasa, S. G. (2019). Principles of Green Roofs Design. *Buletinul Institutului Politehnic Din Iasi*, 63-75.

Besir, A. B., & Cuce, E. (2017). *Green roofs and facades: A comprehensive review.* Elsevier.

Biddle, J. (2008). Explaining the spread of residential air conditioning, 1955–1980. *Explorations in Economic History 45* , 402-423.

Bixler, R. P., & Yang, E. (2020). *Climate Vulnerability in Austin: A multi-risk assessment.* An Austin Area Sustainability Indicators and Planet Texas 2050 Unpublished Technical Report.

Bruse, M., & Fleer, H. (1998). Simulating surface–plant–air interactions inside urban environments with a three dimensional numerical model. *Environmental Modelling & Software 13*, 373-384.

Cascone, S., Catania, F., Gagliano, A., & Sciuto, G. (2018). *A comprehensive study on green roof performance for retrofitting existing buildings.* Catania: Elsevier.

CDC. (2017, June 19). *Center for Disease Control and Prevention*. Retrieved from www.cdc.gov: https://www.cdc.gov/disasters/extremeheat/heat_guide.html

CDC. (n.d.). *Centers for Disease Control and Prevention. National Environmental Public Health Tracking Network.* Retrieved from www.cdc.gov/ephtracking.: https://ephtracking.cdc.gov/DataExplorer/

Census Block Group Map. (2020, 10). *Census Block Group Map.* Retrieved from www.arcgis.com: https://www.arcgis.com/apps/webappviewer/index.html?id=6ee43749c3544b3092ac36f2f2ce8f79

Chan, H.-Y., Riffat, S. B., & Zhu, J. (2009). Review of passive solar heating and cooling technologies. *Renewable and Sustainable Energy Reviews 14*, 781-789.

Chen, J., Augenbroe, G., & Song, X. (2018). Evaluating the potential of hybrid ventilation for small to mediumsized office buildings with different intelligent controls anduncertainties in US climates. *Elsevier: Energy and Buildings 158*, 1648-1661.

Chen, Y., Tong, Z., & Malkawi, A. (2017). Investigating natural ventilation potentials across the globe: Regional and climatic variations. *Elsevier: Building and Environment 122*, 386-396.

CodeNEXT. (2018, April 20). *Code NEXT Shaping the Austin we Imagine*. Retrieved from www.codenext.engagingplans.org: https://www.codenext.engagingplans.org/codenext-comparison-map

de Dear, R. J., & Brager, G. S. (2002). Thermal comfort in naturally ventilated buildings: revisions to ASHRAE Standard 55. *Energy and Buildings 34*, 549-561.

Douglas, I., & James, P. (2015). *Urban Ecology: an Introduction.* London & New York: Routledge.

EIA. (2018). *What's New in How We Use Energy at Home: Results from EIA's 2015 Residential Energy Consumption Survey (RECS).* Washington, DC: U.S. Energy Inormation Administration Independent Statistics & Analysis.

Elsadek, M., Liu, B., & Lian, Z. (2019). *Green façades: Their contribution to stress recovery and well-being in high-density cities.* Elsevier.

EnergyPlus. (n.d.). *EnergyPlus Weather Data*. Retrieved from www.energyplus.net: https://energyplus.net/weather-location/north_and_central_america_wmo_region_4/USA/TX/USA_TX_Austin-Camp.Mabry.722544_TMY3

ENVI-met. (2021, April 22). *ENVI-met.* Retrieved from www.envi-met.com: https://www.envi-met.com/

EPA. (n.d.). *United States Environmental Protection Agency*. Retrieved from epa.gov: https://www.epa.gov/heatislands/learn-about-heat-islands

Ezzeldin, S., & Rees, S. J. (2013). The potential for office buildings with mixed-mode ventilation and low energy cooling systems in arid climates. *Elsevier: Energy and Buildings 65*, 368-381.

Franchini, M., & Mannucci, P. M. (2015). Impact on human health of climate changes. *Elsevier: European Journal of Internal Medicine 26*, 1-5.

Francis, M. (2019, August 28). *www.eia.gov*. Retrieved from EIA updates its U.S. energy consumption by source and sector chart: https://www.eia.gov/todayinenergy/detail.php?id=41093

Givoni, B. (1991). Comfort, climate analysis and building design guidelines. *Energy and Buildings 18*, 11-23.

Green Roofs for Healthy Cities. (2019). *greenroofs.org*. Retrieved from https://greenroofs.org/about-green-roofs

Hartig, T., & Kahn Jr., P. H. (2016). Living in cities, naturally. *Science*, 938-940.

Hawken, P. (2017). *Drawdown The Most Comprehensive Plan Ever Proposed to Reverse Global Warming.* New York, New York: Penguin Books.

Heaviside, C., Macintyre, H., & Vardoulakis, S. (2017). The Urban Heat Island: Implications for Health in a Changing Environment. *Current Environmental Health Reports 4*, pages296–305.

Holopainen, R., Tuomaala, P., Hernandez, P., Häkkinen, T., Piira, K., & Piippo, J. (2013). Comfort assessment in the context of sustainable buildings: Comparison of simplified and detailed human thermal sensation methods. *Building and Environment 71*, 60-70.

Howard, L. (1833). *The Climate of London, deduced from meteorological observations made in the metropolis, and at various places around it. In three volumes.* London: W.Phillips.

Huang, Q., & Lu, Y. (2017). Urban heat island research from 1991 to 2015: a bibliometric analysis. *Theoretical and Applied Climatology volume 131*, 1055–1067.

Huttner, S. (2012). *Further development and application of the 3D microclimate simulation ENVI-met.* Germany: Mainz University.

IPCC. (2013). *Climate Change 2013: The Physical Science Basis.* Cambridge, United Kingdom and New York, NY, USA: Cambridge University Press.

Isaac, M., & vanVuuren, D. P. (2008). Modeling global residential sector energy demand for heating and air conditioning in the context of climate change. *Energy Policy 37*, 507-521.

Izadyar, N., Miller, W., Rismanchi, B., & Garcia-Hansen, V. (2019). Impacts of façade openings' geometry on natural ventilation and occupants' perception: A review. *Elsevier: Building and Environment 170*, 106613.

Jim, C. (2017). *Green roof evolution through exemplars: Germinal prototypes to modern variants.* Hong Kong: Elsevier.

Karl, T. R., Melillo, J. M., & Peterson, a. T. (2009). *Global Climate Change Impacts in the United States.* Cambridge University Press.

Koop, S., Dorssen, A. V., & Brouwer, S. (2019). *Enhancing domestic water conservation behaviour: A review of empirical studies on influencing tactics.* Nieuwegein, Netherlands: Elsevier.

Košir, M. (2019). *Climate Adaptability of Buildings Bioclimatic Design in the Light of Climate Change.* Springer International Publishing.

Li, C., Wei, J., & Li, C. (2019). Influence of foliage thickness on thermal performance of green façades in hot and humid climate. *Elsevier: Energy & Buildings 199*, 72-87.

Lovell, S. T., & Taylor, J. R. (2013). Supplying urban ecosystem services through multifunctional green infrastructure in the United States. *Landscape Ecol*, 1447–1463.

Manso, M., & Castro-Gomes, J. (2014). *Green Wall Systems: a Review of their Characteristics.* Elsevier.

Manzano-Agugliaro, F., Montoya, F. G., Sabio-Ortega, A., & García-Cruz, A. (2015). Review of bioclimatic architecture strategies for achieving thermal comfort. *RenewableandSustainableEnergyReviews 49*, 736-755.

Marcus, J. (2010, July 09). *www.wildflower.org.* Retrieved from Lady Bird Johnson Wildflower Center: https://www.wildflower.org/expert/show.php?id=5939

Mather, L. (2017, Jun 06). *www.architecturaldigest.com.* Retrieved from Architectural Digest - Gardens + Landscapes: https://www.architecturaldigest.com/story/are-climbing-plants-really-bad-for-your-house

Melikov, A. K., & Kaczmarczyk, J. (2012). Air movement and perceived air quality. *Building and Environment 47*, 400-409.

Memon, R. A., Leung, D. Y., & Chunho, L. (2007). A review on the generation, determination and mitigation of Urban Heat Island. *Journal of Environmental Sciences 20*, 120-128.

Morakinyo, T. E., Lai, A., Lau, K. K.-L., & Ng, E. (2019). Thermal benefits of vertical greening in a high-density city: Case study of Hong Kong. *Urban Forestry & Urban Greening 37*, 42-55.

Nagengast, B. (2002). 100 Years of Air Conditioning. *ASHRAE journal 44, no. 6*, 44-46.

NASA. (2020). *Earth Observatory.* Retrieved from earthobservatory.nasa.gov: https://earthobservatory.nasa.gov/world-of-change/global-temperatures

NOAA. (n.d.). *National Weather Service National: Oceanic and Atmospheric Administration*. Retrieved from www.weather.gov: https://www.weather.gov/media/ewx/climate/ClimateSummary-ewx-Austin.pdf

Oke, T. R. (1973). City Size and the Urban Heat Island. *Atmospheric Environment Pergamon Press*, Vol. 7, pp. 769-779.

Oke, T. R. (1982). The Energetic Basis of the Urban Heat Island. *Quarterly Journal of the Royal Meteorological Society*, Vol. 108, pp. 1-24.

Pacheco, R., Ordóñez, J., & Martínez, G. (2012). Energy efficient design of building: A review. *Renewable and Sustainable Energy Reviews 16*, 3559-3573.

Panagiotidou, M., & Fuller, R. J. (2013). Progress in ZEBs — A review of definitions, policies and construction activity. *Energy Policy 62*, 196-206.

Peng, L. L., Jiang, Z., Yang, X., He, Y., Xu, T., & Chen, S. S. (2020). Cooling effects of block-scale facade greening and their relationship with urban form. *Building and Environment 169*, 106552.

Radic, M., Dodig, M. B., & Auer, T. (2019). *Green Facades and Living Walls—A Review Establishing the Classification of Construction Types and Mapping the Benefits.* Basel: Sustainability.

Raji, B., Tenpierik, M. J., & Van Den Dobbelsteen, A. (2015). *The impactofgreeningsystemsonbuildingenergy performance: Aliteraturereview.* Elsevier.

Rouviere, C., Williams, T., Ball, R., Shinyak, Y., Topping, J., Nishioka, S., . . . Okita, T. (1990). 5: Human settlement; the energy, transport and industrial sectors; human health; air quality, and changes in ultraviolet-B radiation . In W. M. Tegart, G.W, S. a. D.C, & Griffiths, *Climate Change: The IPCC Impacts Assessment* (pp. 5.1-5.45). Canberra: Australian Government Publishing Service.

Salcido, J. C., Raheem, A. A., & Issac, R. R. (2016). From simulation to monitoring: Evaluating the potential of mixed-mode ventilation (MMV) systems for integrating natural ventilation in office buildings through a comprehensive literature review. *Energy and Buildings 127*, 1008-1018.

Santamouris, M. (2001). Chapter 5: Heat-Island Effect. In M. Santamouris, D. Asimakopoulos, V. Assimakopoulos, N. Chrisomallidou, N. Klitsikas, D. Mangold, . . . A. Tsangrassoulis, *Energy and Climate in the Urban Built Environment* (pp. 48-68). James & James.

Santamouris, M. (2013). Using cool pavements as a mitigation strategy to fight urban heat island—A review of the actual developments. *Renewable and Sustainable Energy Reviews 26*, 224-240.

Santamouris, M. (2014). On the energy impact of urban heat island and global warming on buildings. *Elsevier: Energy and Buildings 82*, 100-113.

Santamouris, M. (2015). Regulating the damaged thermostat of the cities—Status, impacts andmitigation challenges. *Elsevier: Energy and Buildings 91*, 43-56.

Santamouris, M. (2016). Cooling the buildings – past, present and future. *Energy and Buildings 128*, 617-638.

Santamouris, M. (2019). Recent progress on urban overheating and heat island research. Integrated assessment of the energy, environmental, vulnerability and health impact. Synergies with the global climate change. *Energy & Buildings 207*, 109482.

Schwarz, N., Lautenbach, S., & Seppelt, R. (2011). Exploring indicators for quantifying surface urban heat islands of European cities with MODIS land surface temperatures. *Remote Sensing of Environment*, 115, pp. 3175-3186.

Sedlak, D. (2014). *Water 4.0 The Past, Present, and Future of the World's Most Vital Resource.* New Haven & London: Yale University Press.

Shafique, M., Kim, R., & Rafiq, M. (2018). *Green roof benefits, opportunities and challenges – A review.* Elsevier.

Shah, H. (2019, June 24). *The Unexpected History of the Air Conditioner.* Retrieved from Smithsonian Magazine: https://www.smithsonianmag.com/smithsonian-institution/unexpected-history-air-conditioner-180972108/

Sheng, L., Tang, X., You, H., Gu, Q., & Hu, H. (2016). Comparison of the urban heat island intensity quantified by using air temperature and Landsat land surface temperature in Hangzhou, China. *Ecological Indicators*, Volume 72, Pages 738-746.

Standish, R. J., Hobbs, R. J., & Miller, J. R. (2012). Improving city life: options for ecological restoration in urban landscapes and how these might influence interactions between people and nature. *Landscape Ecol*, 1213–1221.

Sternberg, T., Viles, H., & Cathersides, A. (2010). *Evaluating the role of ivy (Hedera helix) in moderating wall surface microclimates and contributing to the bioprotection of historic buildings.* Elsevier.

Stevanović, S. (2013). Optimization of passive solar design strategies: A review. *Renewable and Sustainable Energy Reviews 25*, 177-196.

Sutton, R. K. (2018). *Green Roofs Increase Structural Loading Costs.* Landscape Architecture Program - University of Nebraska - Lincoln.

Toparlar, Y., Blocken, B., Maiheu, B., & Heijst, G. J. (2017). A review on the CFD analysis of urban microclimate. *Renewable and Sustainable Energy Reviews 80*, 1613-1640.

Tsoka, S., Tsikaloudaki, A., & Theodosiou, T. (2018). Analyzing the ENVI-met microclimate model's performance and assessing cool materials and urban vegetation applications–A review. *Sustainable Cities and Society 43,* 55-76.

Tzikopoulos, A., Karatza, M., & Paravantis, J. (2004). Modeling energy efficiency of bioclimatic buildings. *Energy and Buildings 37,* 529-544.

Tzoulas, K., Korpela, K., Venn, S., Yli-Pelkonen, V., Kazmierczak, A., Niemela, J., & James, P. (2007). Promoting Ecosystem and Human Health in Urban Areas Using Green Infrastructure: A Literature Review. *Landscape and Urban Planning*, 167–178.

U. S. Census Bureau. (2019, May 23). *www.census.gov*. Retrieved from Fastest-Growing Cities Primarily in the South and West: https://www.census.gov/newsroom/press-releases/2019/subcounty-population-estimates.html

U.S. Census Bureau. (2020, May). *www.census.gov.* Retrieved from Annual Estimates of the Resident Population for Incorporated Places in the United States: April 1, 2010 to July 1, 2019 (SUB-IP-EST2019-ANNRES): https://www.census.gov/data/tables/time-series/demo/popest/2010s-total-cities-and-towns.html#tableshttps://www.census.gov/data/tables/time-series/demo/popest/2010s-total-cities-and-towns.html#tables

United Nations. (2018, May 16). *un.org*. Retrieved from https://www.un.org/development/desa/en/news/population/2018-revision-of-world-urbanization-prospects.html

United Nations. (2019). *www.un.org*. Retrieved from https://www.un.org/en/sections/issues-depth/water/

USGS. (2019). *USGS Science for a changing world*. Retrieved from usgs.gov: https://www.usgs.gov/media/images/urban-heat-islands

Vanos, J. K., Warland, J. S., Gillespie, T. J., & Kenny, N. A. (2010). Review of the physiology of human thermal comfort while exercising in urban landscapes and implications for bioclimatic design. *International Journal of Biometeorology 54*, 319-334.

Veselý, M., & Zeiler, W. (2014). Personalized conditioning and its impact on thermal comfortand energy performance–A review. *Renewable and Sustainable Energy Reviews 34*, 401-408.

Vijayaraghavan, K. (2016). *Greenroofs:Acriticalreviewontheroleofcomponents,benefits, limitations andtrends.* Chennai: Elsevier.

Voogt, J. A., & Oke, T. R. (2003). Thermal remote sensing of urban climates. *Remote Sensing of Environment*, Volume 86, Issue 3, Pages 370-384.

Ward, K., Lauf, S., Kleinschmit, B., & Endlicher, W. (2016). Heat waves and urban heat islands in Europe: A review of relevant drivers. *Elsevier: Science of the Total Environment*, 527–539.

Ward, N. (2009). *The University of Texas at Austin Texas Scholar Work.* Retrieved from Austin Climate Data, Center for Sustainable Development, The University of Texas at Austin School of Architecture:

https://repositories.lib.utexas.edu/bitstream/handle/2152/11697/3-Ward-Austin_Climate_Data.pdf?sequence=2&isAllowed=y

WHO. (2018, June 1). *www.who.int.* Retrieved from World Health Organization: https://www.who.int/news-room/fact-sheets/detail/climate-change-heat-and-health

Woodward, M., & Berry, C. (2018, June 5). *www.eia.gov*. Retrieved from EIA's residential energy survey now includes estimates for more than 20 new end uses: https://www.eia.gov/todayinenergy/detail.php?id=36412&src=%E2%80%B9%20 Consumption%20%20%20%20%20%20Residential%20Energy%20Consumption %20Survey%20(RECS)-b3

Yamazaki, D., Ikeshima, D., Tawatari, R., Yamaguchi, T., O'Loughlin, F., Neal, J. C., . . . Bates, P. D. (2017, May 31). *Elevation Data: A high-accuracy map of global terrain elevations*. Retrieved from en-us.topographic-map.com: https://en-us.topographic-map.com/maps/ndx/Austin/

Yow, D. M. (2007). Urban Heat Islands: Observations, Impacts, and Adaptation. *Geography Compass 1/6*, 1227–1251.

Permanent address (or email): maitebizcar@gmail.com

This dissertation was typed by Maite Bizcarguenaga Doucet